Structure and reactions of light nuclei studied in fermionic molecular dynamics

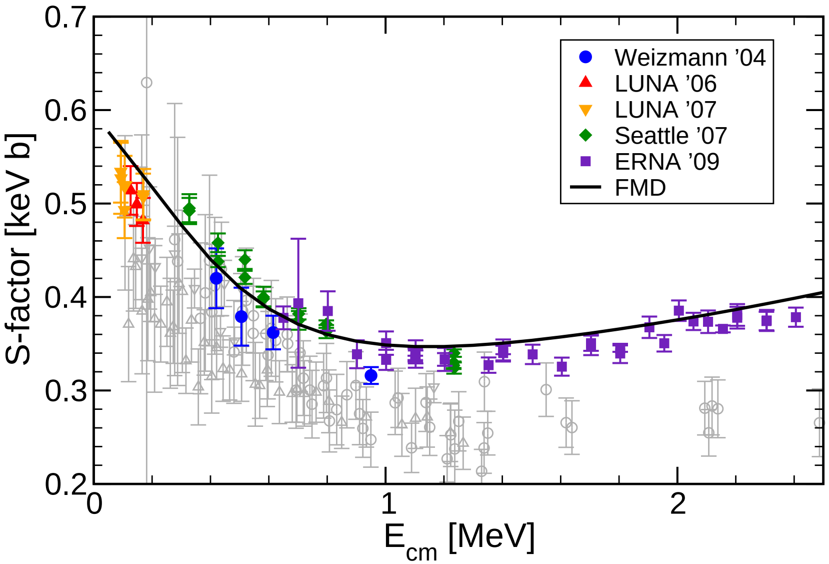

Thomas Neff

"Astrophysics and Nuclear Structure"

International Workshop XLI
on Gross Properties of
Nuclei and Nuclear Excitations

Hirschegg, Austria

January 26 - February 1, 2013

Overview

Realistic Effective Nucleon-Nucleon interaction:

Unitary Correlation Operator Method

R. Roth, T. Neff, H. Feldmeier, Prog. Part. Nucl. Phys. 65 (2010) 50

- **Short-range Correlations and Effective Interaction**

Many-Body Approach:

Fermionic Molecular Dynamics

- **Model**
- **^{3}He(α,γ)^{7}Be Radiative Capture Reaction**

T. Neff, Phys. Rev. Lett. 106, 042502 (2011)

- **Beryllium Isotopes**

A. Krieger *et al.*, Phys. Rev. Lett. 108, 142501 (2012)

Nuclear Force

Argonne V18 (T=0)

spins aligned parallel or perpendicular to the relative distance vector

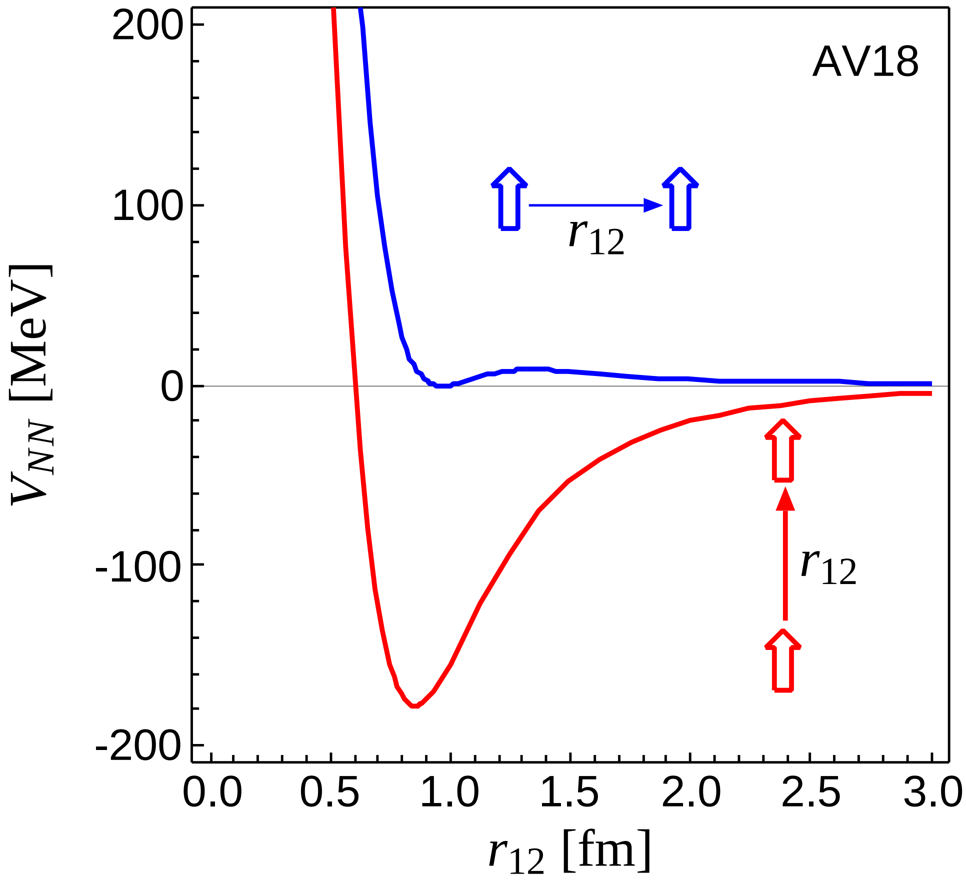

- strong repulsive core: nucleons can not get closer than ≈ 0.5 fm

➽ **central correlations**

- strong dependence on the orientation of the spins due to the tensor force

➽ **tensor correlations**

Nuclear Force

Argonne V18 (T=0)

spins aligned parallel or perpendicular to the relative distance vector

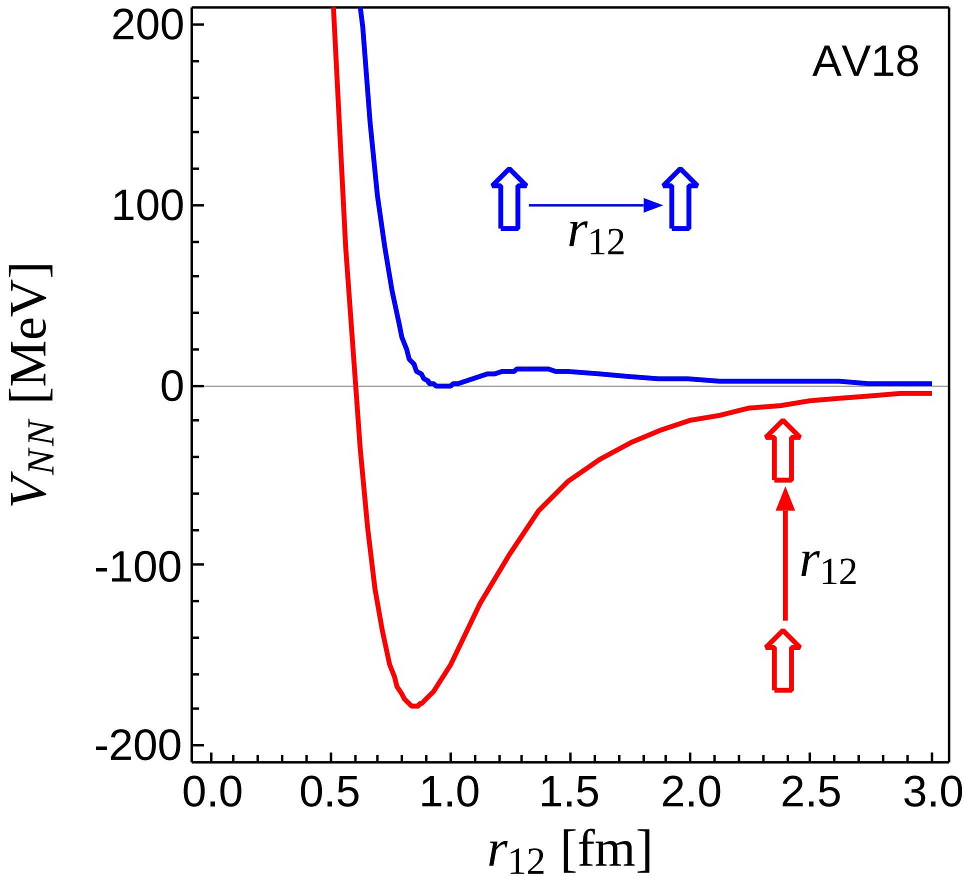

- strong repulsive core: nucleons can not get closer than ≈ 0.5 fm

➽ **central correlations**

- strong dependence on the orientation of the spins due to the tensor force

➽ **tensor correlations**

the nuclear force will induce **strong short-range correlations** in the nuclear wave function

Two-body densities in $A = 2, 3, 4$ Nuclei — AV8'

coordinate space
$S = 1, M_S = 1$, $T = 0$

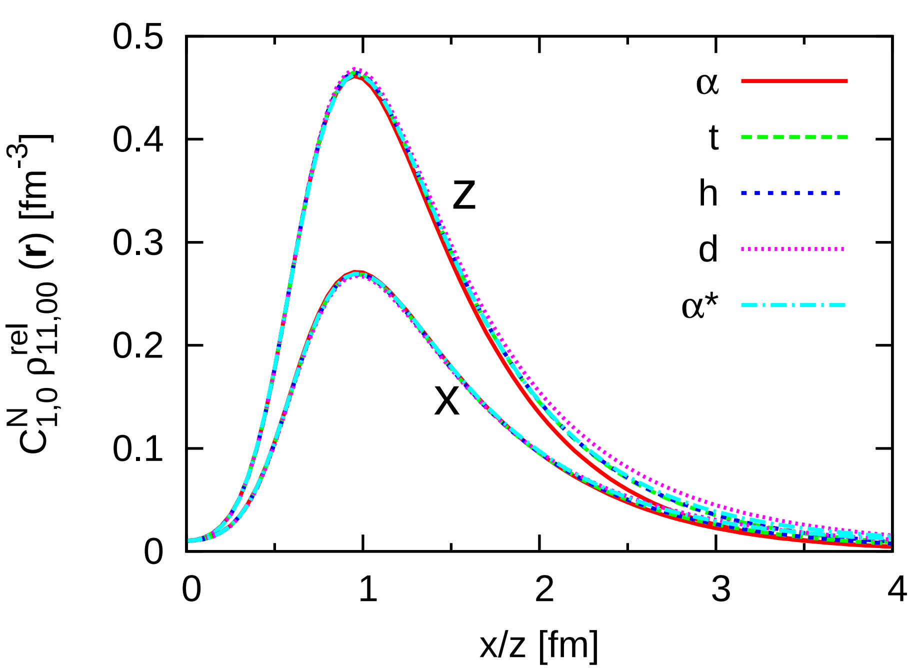

momentum space
$S = 1$, $T = 0$

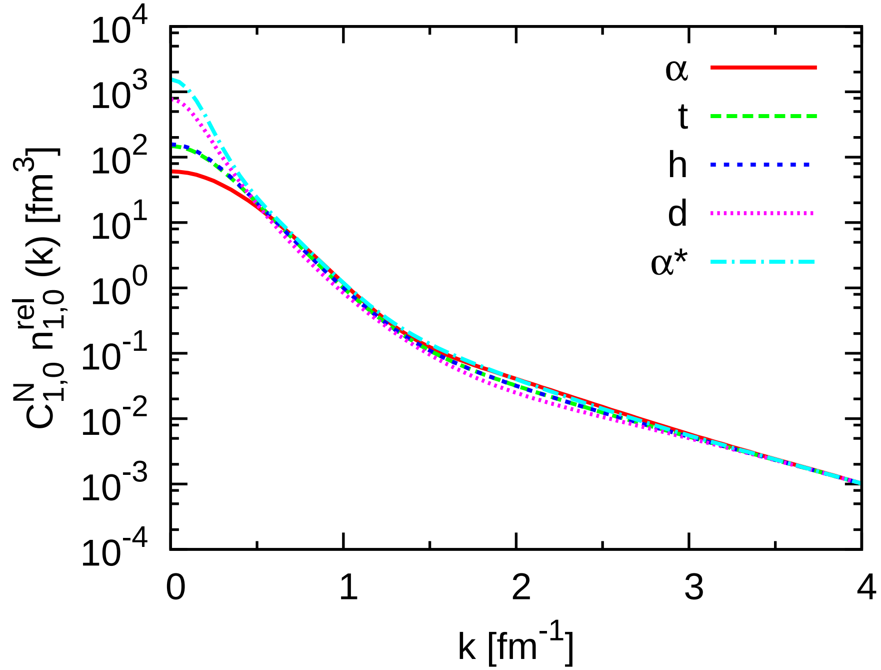

- normalize two-body density in coordinate space at r=1.0 fm
- normalized two-body densities in coordinate space are identical at short distances for all nuclei
- use the **same** normalization factor in momentum space – high momentum tails agree for all nuclei

Feldmeier, Horiuchi, Neff, Suzuki, Phys. Rev. C **84**, 054003 (2011)

Unitary Correlation Operator Method

Correlation Operator

- induce short-range (two-body) central and tensor correlations into the many-body state

$$\underset{\sim}{C} = \underset{\sim}{C}_\Omega \underset{\sim}{C}_r = \exp\Big[-i\sum_{i<j} \underset{\sim}{g}_{\Omega,ij}\Big] \exp\Big[-i\sum_{i<j} \underset{\sim}{g}_{r,ij}\Big] \quad , \quad \underset{\sim}{C}^\dagger \underset{\sim}{C} = \underset{\sim}{1}$$

- correlation operator should conserve the symmetries of the Hamiltonian and should be of finite-range, correlated interaction **phase shift equivalent** to bare interaction by construction

Correlated Operators

- correlated operators will have contributions in higher cluster orders

$$\underset{\sim}{C}^\dagger \underset{\sim}{O} \underset{\sim}{C} = \underset{\sim}{\hat{O}}^{[1]} + \underset{\sim}{\hat{O}}^{[2]} + \underset{\sim}{\hat{O}}^{[3]} + \ldots$$

- two-body approximation: correlation range should be small compared to mean particle distance

Correlated Interaction

$$\underset{\sim}{C}^\dagger \left(\underset{\sim}{T} + \underset{\sim}{V}\right) \underset{\sim}{C} = \underset{\sim}{T} + \underset{\sim}{V}_{\mathrm{UCOM}} + \underset{\sim}{V}_{\mathrm{UCOM}}^{[3]} + \ldots$$

Central and Tensor Correlations

$$\underset{\sim}{C} = \underset{\sim}{C}_{\Omega} \underset{\sim}{C}_{r}$$

$$\mathbf{p} = \mathbf{p}_r + \mathbf{p}_\Omega$$

$$\mathbf{p}_r = \frac{1}{2}\left\{\frac{\mathbf{r}}{r}\left(\frac{\mathbf{r}}{r}\mathbf{p}\right) + \left(\mathbf{p}\frac{\mathbf{r}}{r}\right)\frac{\mathbf{r}}{r}\right\}, \qquad \mathbf{p}_\Omega = \frac{1}{2r}\left\{\mathbf{l} \times \frac{\mathbf{r}}{r} - \frac{\mathbf{r}}{r} \times \mathbf{l}\right\}$$

Central and Tensor Correlations

$$\underset{\sim}{C} = \underset{\sim}{C}_\Omega \underset{\sim}{C}_r$$

$$\mathbf{p} = \mathbf{p}_r + \mathbf{p}_\Omega$$

$$\mathbf{p}_r = \frac{1}{2}\left\{\frac{\mathbf{r}}{r}\left(\frac{\mathbf{r}}{r}\mathbf{p}\right) + \left(\mathbf{p}\frac{\mathbf{r}}{r}\right)\frac{\mathbf{r}}{r}\right\}, \qquad \mathbf{p}_\Omega = \frac{1}{2r}\left\{\mathbf{l} \times \frac{\mathbf{r}}{r} - \frac{\mathbf{r}}{r} \times \mathbf{l}\right\}$$

Central Correlations

$$\underset{\sim}{c}_r = \exp\left\{-\frac{i}{2}\{p_r s(r) + s(r) p_r\}\right\}$$

- probability density shifted out of the repulsive core

$S=0, T=1$

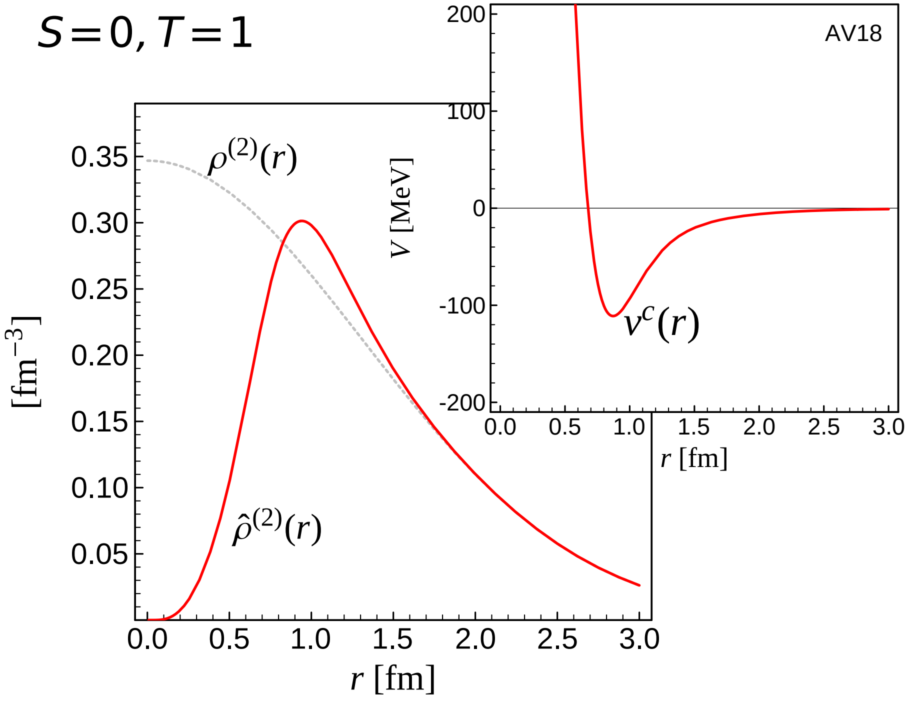

Central and Tensor Correlations

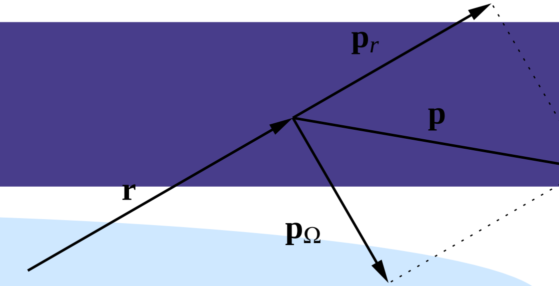

$$\underset{\sim}{C} = \underset{\sim}{C}_\Omega \underset{\sim}{C}_r$$

$$\mathbf{p} = \mathbf{p}_r + \mathbf{p}_\Omega$$

$$\mathbf{p}_r = \frac{1}{2}\left\{\frac{\mathbf{r}}{r}\left(\frac{\mathbf{r}}{r}\mathbf{p}\right) + \left(\mathbf{p}\frac{\mathbf{r}}{r}\right)\frac{\mathbf{r}}{r}\right\}, \qquad \mathbf{p}_\Omega = \frac{1}{2r}\left\{\mathbf{l} \times \frac{\mathbf{r}}{r} - \frac{\mathbf{r}}{r} \times \mathbf{l}\right\}$$

Central Correlations

$$\underset{\sim}{c}_r = \exp\left\{-\frac{i}{2}\{p_r s(r) + s(r) p_r\}\right\}$$

- probability density shifted out of the repulsive core

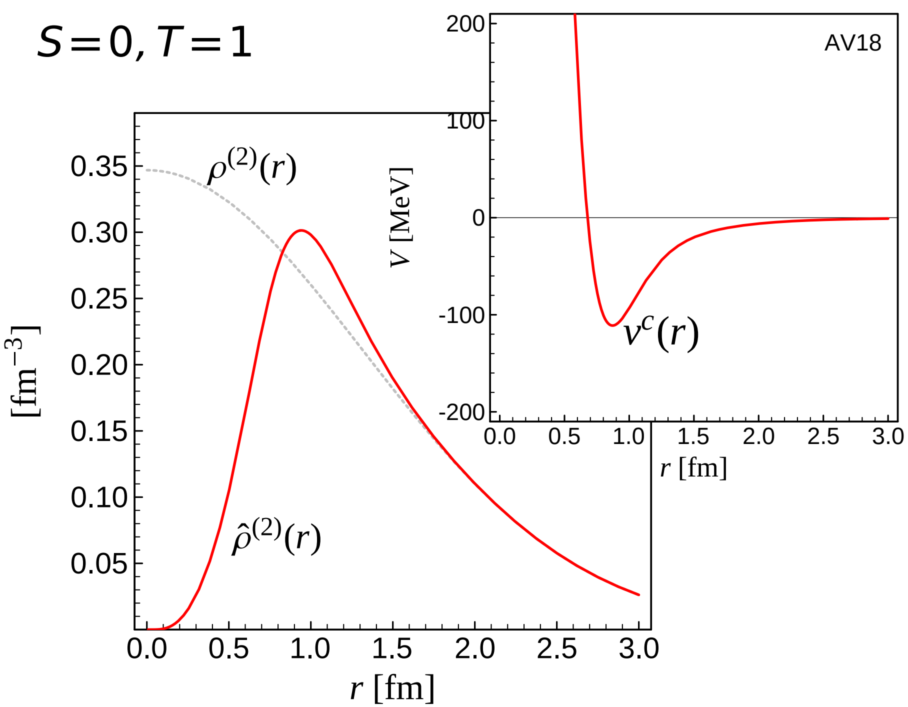

Tensor Correlations

$$\underset{\sim}{c}_\Omega = \exp\left\{-i\vartheta(r)\left\{\frac{3}{2}(\boldsymbol{\sigma}_1\cdot\mathbf{p}_\Omega)(\boldsymbol{\sigma}_2\cdot\mathbf{r}) + \frac{3}{2}(\boldsymbol{\sigma}_1\cdot\mathbf{r})(\boldsymbol{\sigma}_2\cdot\mathbf{p}_\Omega)\right\}\right\}$$

- tensor force admixes other angular momenta

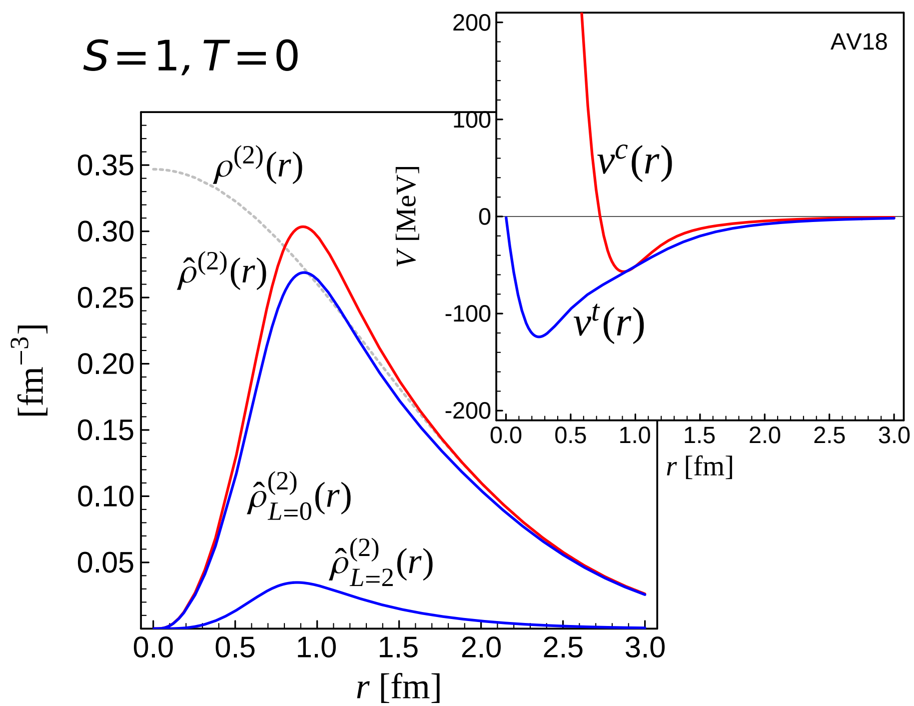

Central and Tensor Correlations

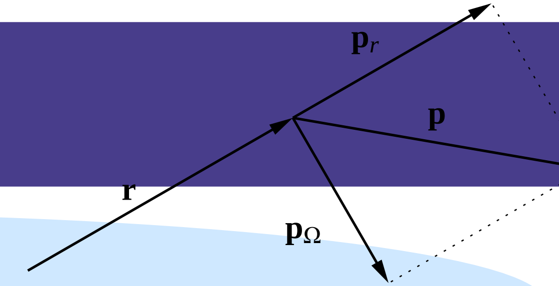

$$\underset{\sim}{C} = \underset{\sim}{C}_\Omega \underset{\sim}{C}_r$$

$$\mathbf{p} = \mathbf{p}_r + \mathbf{p}_\Omega$$

$$\mathbf{p}_r = \frac{1}{2}\left\{\frac{\mathbf{r}}{r}\left(\frac{\mathbf{r}}{r}\mathbf{p}\right) + \left(\mathbf{p}\frac{\mathbf{r}}{r}\right)\frac{\mathbf{r}}{r}\right\}, \qquad \mathbf{p}_\Omega = \frac{1}{2r}\left\{\mathbf{l} \times \frac{\mathbf{r}}{r} - \frac{\mathbf{r}}{r} \times \mathbf{l}\right\}$$

Central Correlations

$$\underset{\sim}{c}_r = \exp\left\{-\frac{i}{2}\{p_r s(r) + s(r) p_r\}\right\}$$

- probability density shifted out of the repulsive core

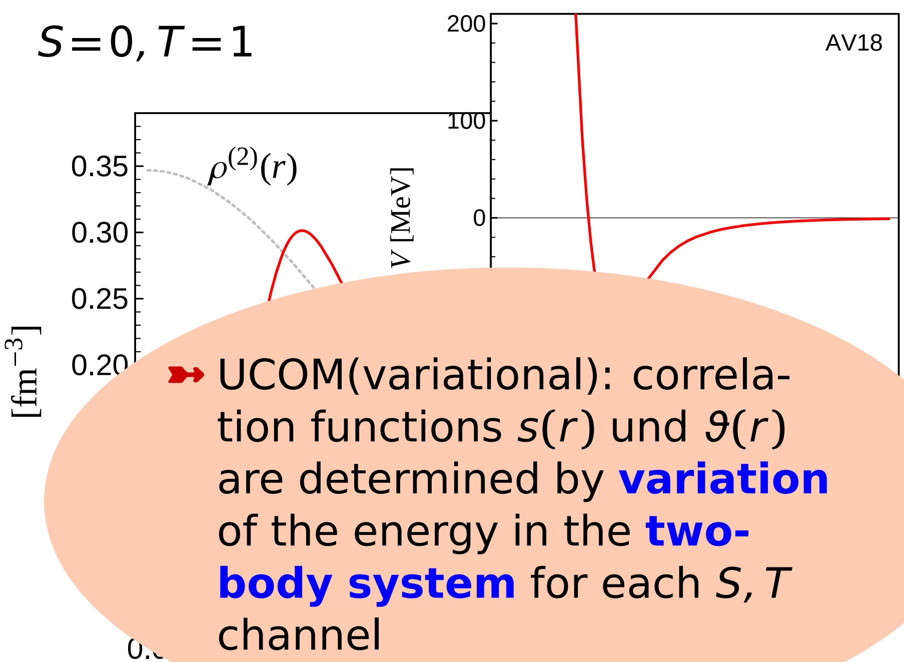

- UCOM(variational): correlation functions $s(r)$ und $\vartheta(r)$ are determined by **variation** of the energy in the **two-body system** for each S, T channel

Tensor Correlations

$$\underset{\sim}{c}_\Omega = \exp\left\{-i\vartheta(r)\left\{\frac{3}{2}(\boldsymbol{\sigma}_1\cdot\mathbf{p}_\Omega)(\boldsymbol{\sigma}_2\cdot\mathbf{r}) + \frac{3}{2}(\boldsymbol{\sigma}_1\cdot\mathbf{r})(\boldsymbol{\sigma}_2\cdot\mathbf{p}_\Omega)\right\}\right\}$$

- tensor force admixes other angular momenta

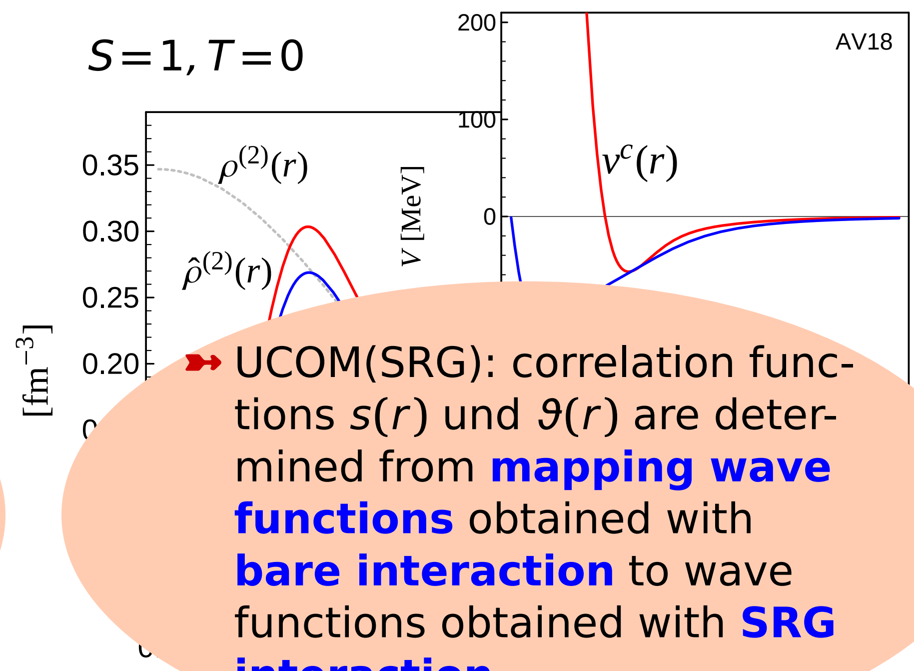

- UCOM(SRG): correlation functions $s(r)$ und $\vartheta(r)$ are determined from **mapping wave functions** obtained with **bare interaction** to wave functions obtained with **SRG interaction**

Correlations and Energies

two-body densities

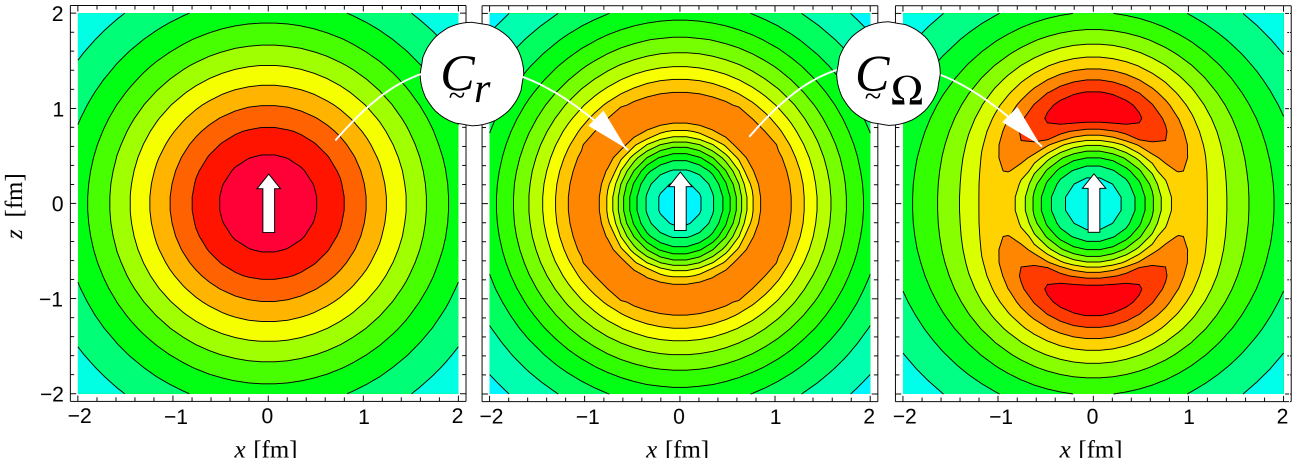

$\rho^{(2)}_{S,T}(\mathbf{r}_1 - \mathbf{r}_2) \quad S=1, M_S=1, T=0$

central correlator $\underset{\sim}{C}_{\mathbf{r}}$ shifts density out of the repulsive core

tensor correlator $\underset{\sim}{C}_{\mathbf{\Omega}}$ aligns density with spin orientation

Neff and Feldmeier, Nucl. Phys. **A713** (2003) 311

Correlations and Energies

two-body densities

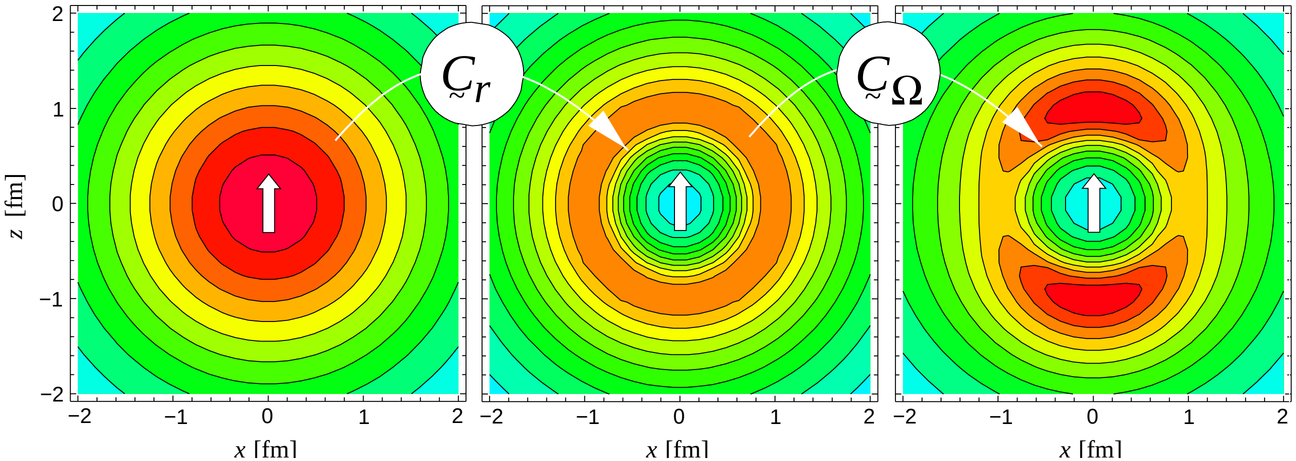

$\rho^{(2)}_{S,T}(\mathbf{r}_1 - \mathbf{r}_2) \quad S = 1, M_S = 1, T = 0$

central correlator $\underset{\sim}{C}_{\mathbf{r}}$
shifts density out of the repulsive core

tensor correlator $\underset{\sim}{C}_{\mathbf{\Omega}}$
aligns density with spin orientation

energies

$0\hbar\omega$ Harmonic Oscillator

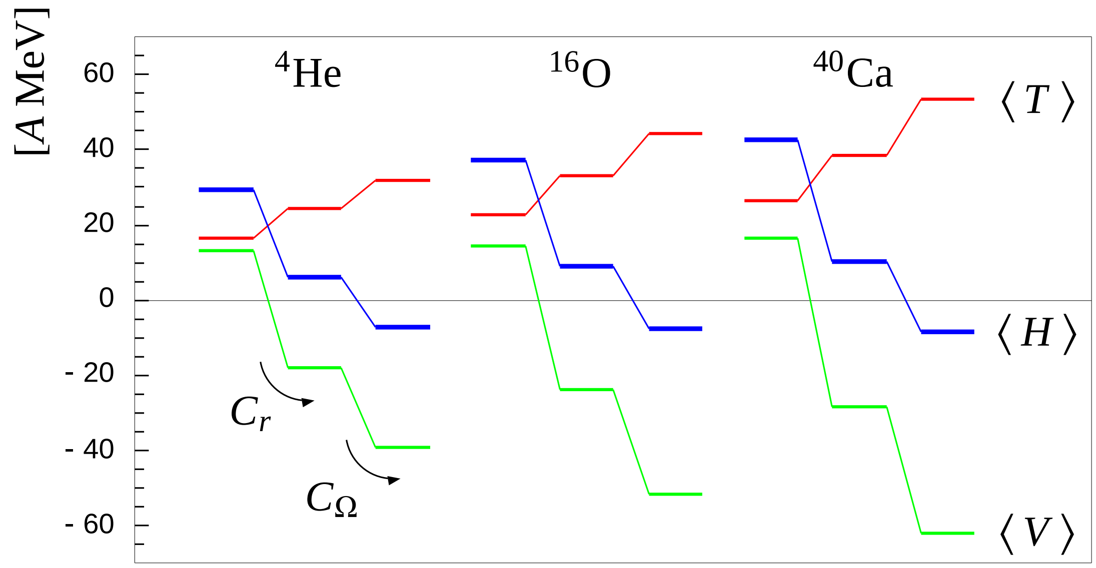

both central and tensor correlations are essential for binding

Neff and Feldmeier, Nucl. Phys. **A713** (2003) 311

Correlated Interaction in Momentum Space

$^3S_1$ bare

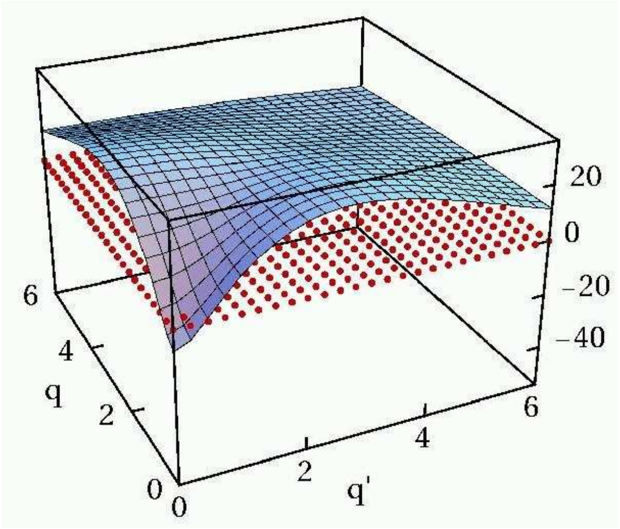

bare interaction has **strong off-diagonal** matrix elements connecting to high momenta

$^3S_1$ - $^3D_1$ bare

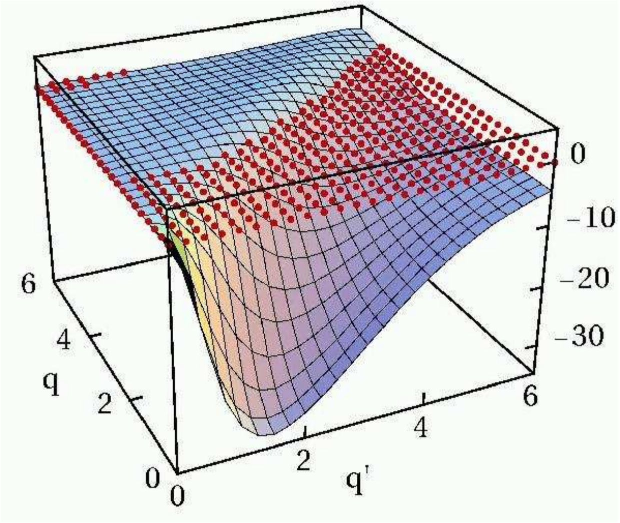

Roth, Hergert, Papakonstaninou, Neff, Feldmeier, Phys. Rev. C **72**, 034002 (2005)

Correlated Interaction in Momentum Space

$^3S_1$ bare

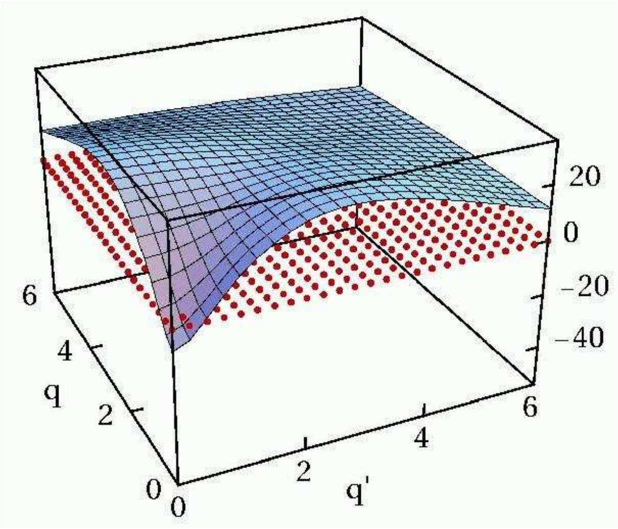

bare interaction has **strong off-diagonal** matrix elements connecting to high momenta

$^3S_1$ - $^3D_1$ bare

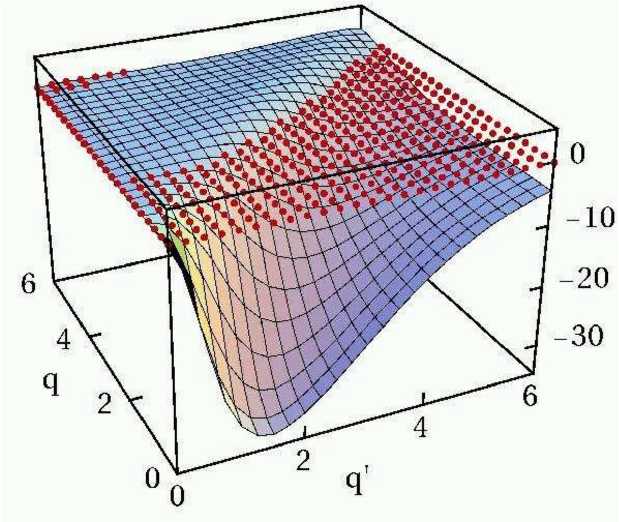

correlated interaction is **more attractive** at low momenta

$^3S_1$ correlated

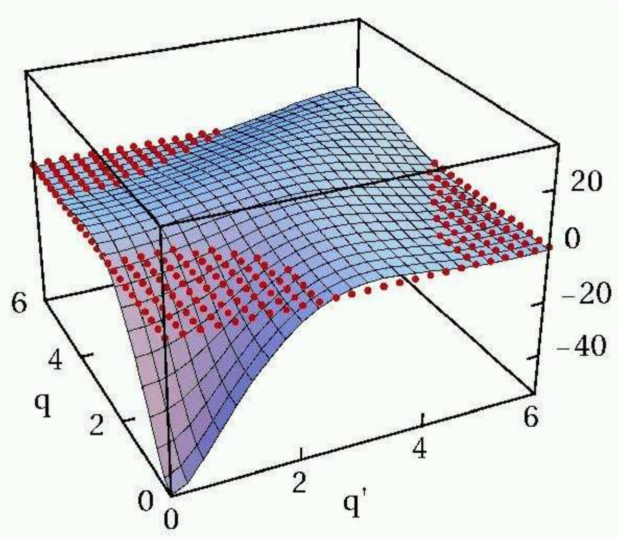

$^3S_1$ - $^3D_1$ correlated

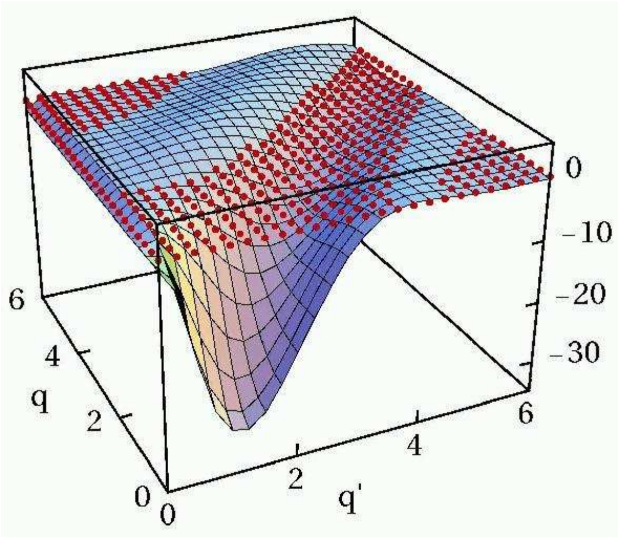

off-diagonal matrix elements connecting low- and high- momentum states are **strongly reduced**

Roth, Hergert, Papakonstaninou, Neff, Feldmeier, Phys. Rev. C **72**, 034002 (2005)

Correlated Interaction in Momentum Space

$^3S_1$ bare

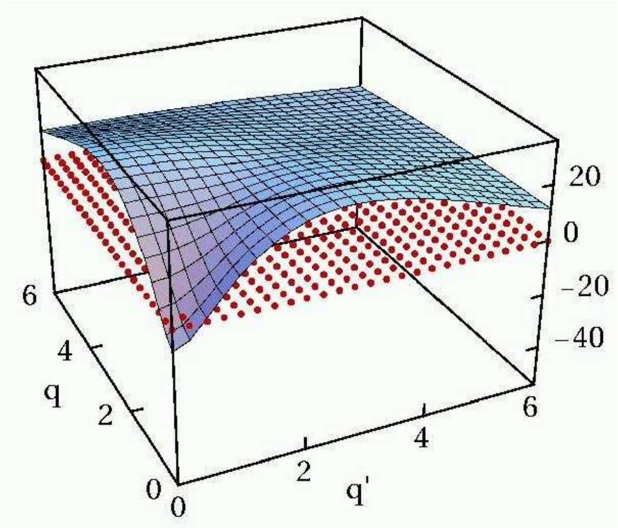

bare interaction has **strong off-diagonal** matrix elements connecting to high momenta

$^3S_1$ - $^3D_1$ bare

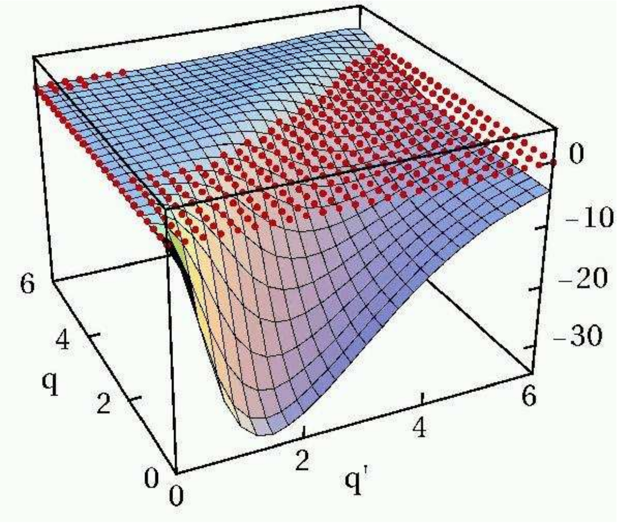

correlated interaction is **more attractive** at low momenta

$^3S_1$ correlated

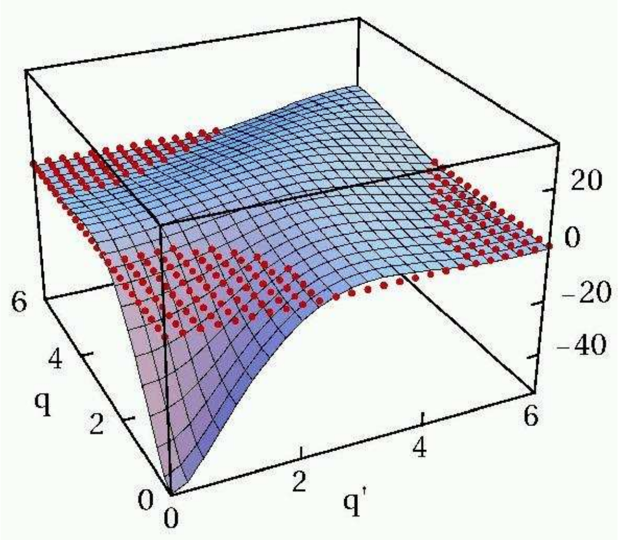

off-diagonal matrix elements connecting low- and high- momentum states are **strongly reduced**

$^3S_1$ - $^3D_1$ correlated

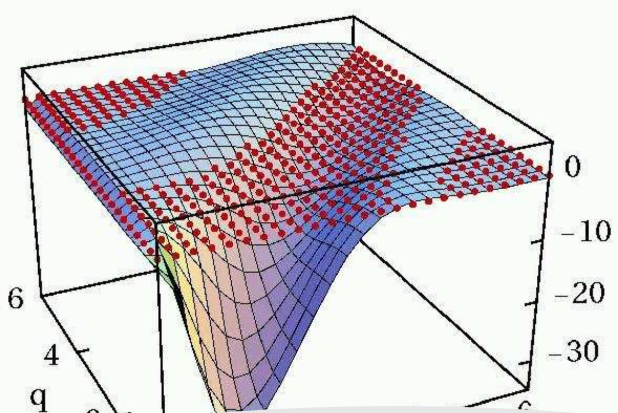

similar to $V_{low\text{-}k}$, **SRG**

Roth, Hergert, Papakonstaninou, Neff, Feldmeier, Phys. Rev. C **72**, 034002 (2005)

No-Core Shell Model Calculations

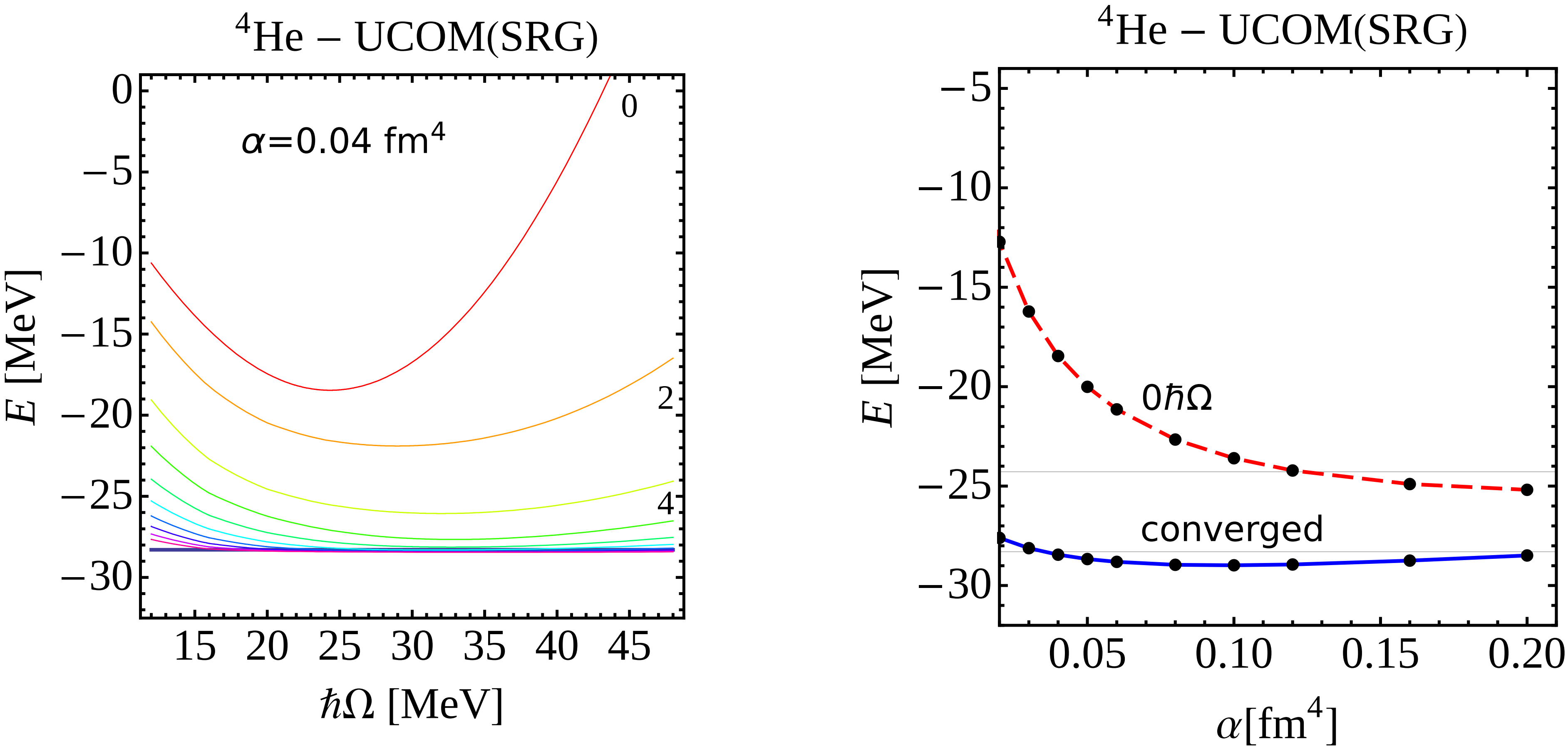

- convergence much improved compared to bare interaction
- effective interaction – in two-body approximation – converges to different energy then bare interaction
- transformed interaction can be tuned to obtain simultaneously (almost) exact ^{3}He and ^{4}He binding energies

Roth, Neff, Feldmeier, Prog. Part. Nucl. Phys. **65**, 50 (2010)

NCSM ^{6}Li/^{7}Li ground state energy

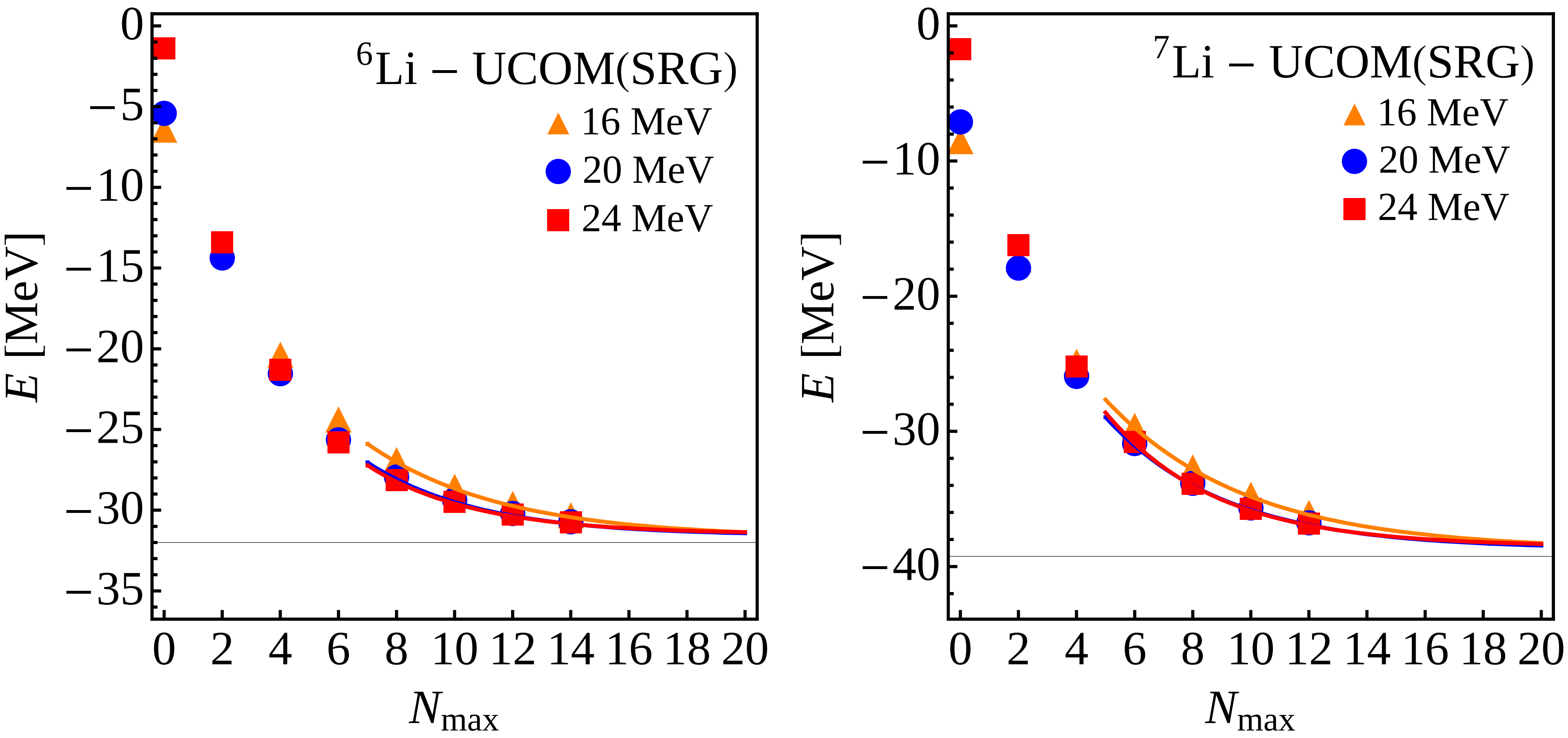

- effective two-body interaction also works reasonably well for (slightly) heavier nuclei

Exotica: Special Challenges

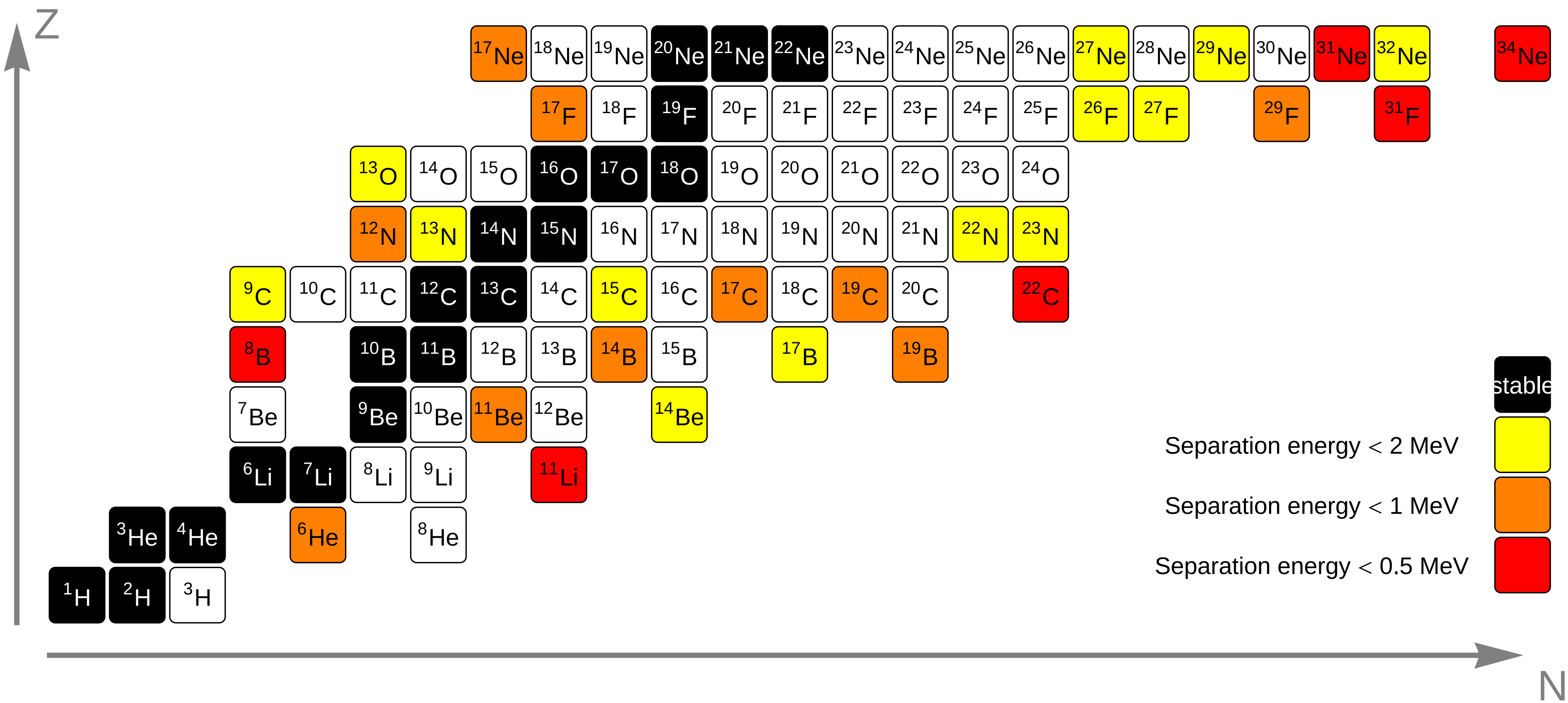

- states close to one-nucleon, two-nucleon or cluster thresholds can have well developed **halo** or **cluster** structure
- these are hard to tackle in the harmonic oscillator basis

Fermionic Molecular Dynamics

Fermionic

Slater determinant

$$\left| Q \right\rangle = \underset{\sim}{\mathcal{A}} \Big(\left| q_1 \right\rangle \otimes \cdots \otimes \left| q_A \right\rangle \Big)$$

- antisymmetrized A-body state

Feldmeier, Schnack, Rev. Mod. Phys. **72** (2000) 655

Neff, Feldmeier, Nucl. Phys. **A738** (2004) 357

Fermionic Molecular Dynamics

Fermionic

Slater determinant

$$\left| Q \right\rangle = \underset{\sim}{\mathcal{A}} \left(\left| q_1 \right\rangle \otimes \cdots \otimes \left| q_A \right\rangle \right)$$

- antisymmetrized A-body state

Molecular

single-particle states

$$\left\langle \mathbf{x} \middle| q \right\rangle = \sum_i c_i \exp\left\{ -\frac{(\mathbf{x} - \mathbf{b}_i)^2}{2a_i} \right\} \otimes \left| \chi^\uparrow_i, \chi^\downarrow_i \right\rangle \otimes \left| \xi \right\rangle$$

- Gaussian wave-packets in phase-space (complex parameter $\mathbf{b}_i$ encodes mean position and mean momentum), spin is free, isospin is fixed
- width a_i is an independent variational parameter for each wave packet
- use one or two wave packets for each single particle state

Feldmeier, Schnack, Rev. Mod. Phys. **72** (2000) 655

Neff, Feldmeier, Nucl. Phys. **A738** (2004) 357

Fermionic Molecular Dynamics

Fermionic

Slater determinant

$$\left| Q \right\rangle = \underset{\sim}{\mathcal{A}} \left(\left| q_1 \right\rangle \otimes \cdots \otimes \left| q_A \right\rangle \right)$$

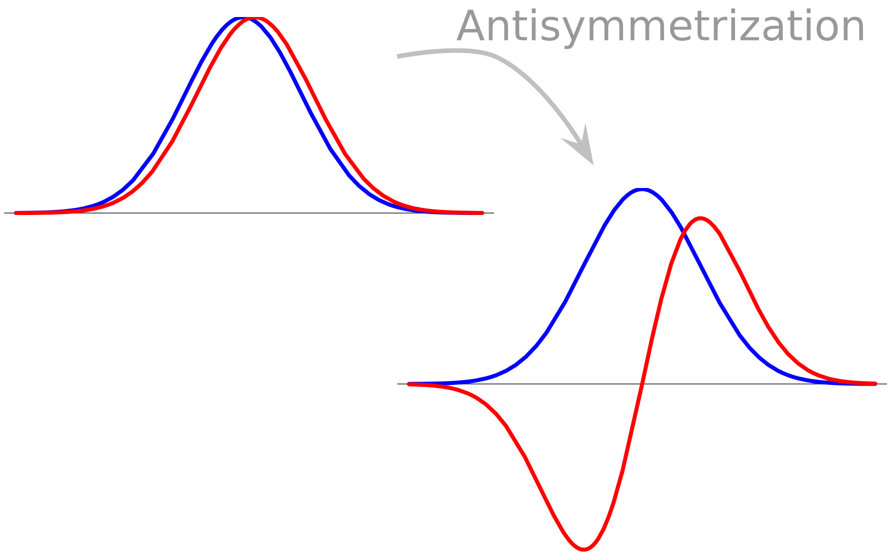

- antisymmetrized A-body state

Molecular

single-particle states

$$\left\langle \mathbf{x} \middle| q \right\rangle = \sum_i c_i \exp\left\{ -\frac{(\mathbf{x} - \mathbf{b}_i)^2}{2a_i} \right\} \otimes \left| \chi^{\uparrow}_i, \chi^{\downarrow}_i \right\rangle \otimes \left| \xi \right\rangle$$

- Gaussian wave-packets in phase-space (complex parameter $\mathbf{b}_i$ encodes mean position and mean momentum), spin is free, isospin is fixed
- width a_i is an independent variational parameter for each wave packet
- use one or two wave packets for each single particle state

Feldmeier, Schnack, Rev. Mod. Phys. **72** (2000) 655

Neff, Feldmeier, Nucl. Phys. **A738** (2004) 357

Fermionic Molecular Dynamics

Fermionic

Slater determinant

$$\left| Q \right\rangle = \underset{\sim}{\mathcal{A}}\left(\left| q_1 \right\rangle \otimes \cdots \otimes \left| q_A \right\rangle \right)$$

- antisymmetrized A-body state

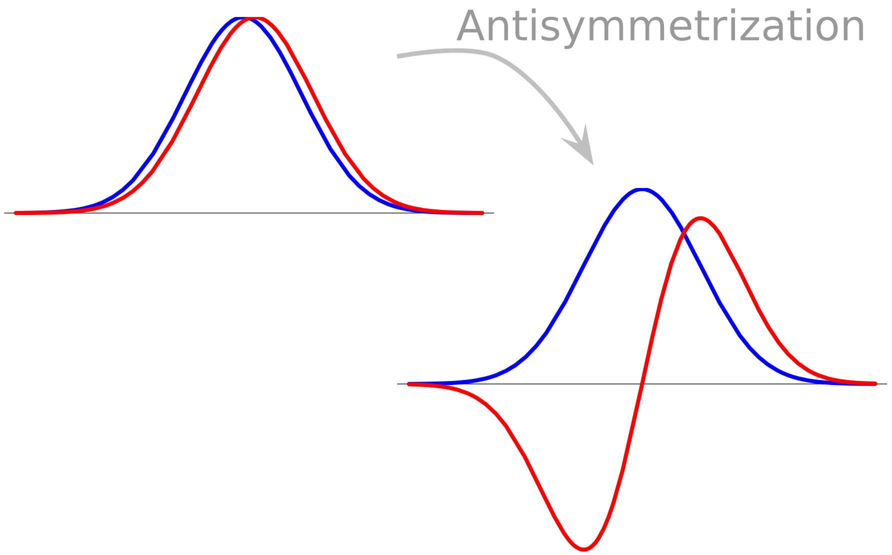

Molecular

single-particle states

$$\left\langle \mathbf{x} \middle| q \right\rangle = \sum_i c_i \exp\left\{ -\frac{(\mathbf{x} - \mathbf{b}_i)^2}{2a_i} \right\} \otimes \left| \chi^\uparrow_i, \chi^\downarrow_i \right\rangle \otimes \left| \xi \right\rangle$$

- Gaussian wave-packets in phase-space (complex parameter $\mathbf{b}_i$ encodes mean position and mean momentum), spin is free, isospin is fixed
- width a_i is an independent variational parameter for each wave packet
- use one or two wave packets for each single particle st

see also
Antisymmetrized Molecular Dynamics
Horiuchi, Kanada-En'yo, Kimura, . . .

Feldmeier, Schnack, Rev. Mod. Phys. **72** (2000) 655

Neff, Feldmeier, Nucl. Phys. **A738** (2004) 357

Interaction Matrix Elements

(One-body) Kinetic Energy

$$\langle q_k | \underset{\sim}{T} | q_l \rangle = \langle a_k \mathbf{b}_k | \underset{\sim}{T} | a_l \mathbf{b}_l \rangle \langle \chi_k | \chi_l \rangle \langle \xi_k | \xi_l \rangle$$

$$\langle a_k \mathbf{b}_k | \underset{\sim}{T} | a_l \mathbf{b}_l \rangle = \frac{1}{2m} \left(\frac{3}{a_k^\star + a_l} - \frac{(\mathbf{b}_k^\star - \mathbf{b}_l)^2}{(a_k^\star + a_l)^2} \right) R_{kl}$$

$$\alpha_{klmn} = \frac{a_k{}^\star a_m}{a_k{}^\star + a_m} + \frac{a_l{}^\star a_n}{a_l{}^\star + a_n}$$

$$\rho_{klmn} = \frac{a_m \mathbf{b}_k{}^\star + a_k{}^\star \mathbf{b}_m}{a_k{}^\star + a_m} - \frac{a_n \mathbf{b}_l{}^\star + a_l{}^\star \mathbf{b}}{a_l{}^\star + a_n}$$

$$R_{km} = \langle a_k \mathbf{b}_k | a_m \mathbf{b}_m \rangle$$

(Two-body) Potential

- fit radial dependencies by (a sum of) Gaussians

$$G(\mathbf{x}_1 - \mathbf{x}_2) = \exp\left\{ -\frac{(\mathbf{x}_1 - \mathbf{x}_2)^2}{2\kappa} \right\}$$

- Gaussian integrals

$$\langle a_k \mathbf{b}_k, a_l \mathbf{b}_l | \underset{\sim}{G} | a_m \mathbf{b}_m, a_n \mathbf{b}_n \rangle = R_{km} R_{ln} \left(\frac{\kappa}{\alpha_{klmn} + \kappa} \right)^{3/2} \exp\left\{ -\frac{\rho_{klmn}^2}{2(\alpha_{klmn} + \kappa)} \right\}$$

- analytical expressions for matrix elements

Operator Representation of V_{UCOM}

$$\underset{\sim}{C}^{\dagger}(\underset{\sim}{T}+\underset{\sim}{V})\underset{\sim}{C} \quad = \quad \underset{\sim}{T}$$

one-body kinetic energy

$$+\sum_{ST} \hat{V}_{c}^{ST}(r) + \frac{1}{2}\left(\underset{\sim}{p_r}^2\, \hat{V}_{p^2}^{ST}(r) + \hat{V}_{p^2}^{ST}(r)\,\underset{\sim}{p_r}^2\right) + \hat{V}_{l^2}^{ST}(r)\,\underset{\sim}{\mathbf{l}}^2$$

central potentials

$$+\sum_{T} \hat{V}_{ls}^{T}(r)\,\underset{\sim}{\mathbf{l}}\cdot\underset{\sim}{\mathbf{s}} + \hat{V}_{l^2 ls}^{T}(r)\,\underset{\sim}{\mathbf{l}}^2\,\underset{\sim}{\mathbf{l}}\cdot\underset{\sim}{\mathbf{s}}$$

spin-orbit potentials

$$+\sum_{T} \hat{V}_{t}^{T}(r)\,\underset{\sim}{S}_{12}(\mathbf{r},\mathbf{r}) + \hat{V}_{trp_\Omega}^{T}(r)\,\underset{\sim}{p_r}\,\underset{\sim}{S}_{12}(\mathbf{r},\mathbf{p_\Omega}) + \hat{V}_{tll}^{T}(r)\,\underset{\sim}{S}_{12}(\mathbf{l},\mathbf{l}) +$$
$$\hat{V}_{tp_\Omega p_\Omega}^{T}(r)\,\underset{\sim}{S}_{12}(\mathbf{p_\Omega},\mathbf{p_\Omega}) + \hat{V}_{l^2 tp_\Omega p_\Omega}^{T}(r)\,\underset{\sim}{\mathbf{l}}^2\underset{\sim}{S}_{12}(\mathbf{p_\Omega},\mathbf{p_\Omega})$$

tensor potentials

bulk of tensor force mapped onto central part
of correlated interaction

tensor correlations also change the spin-orbit
part of the interaction

Nucl. Phys. **A745** (2004) 3

PAV, VAP and Multiconfiguration

Projection After Variation (PAV)

- mean-field may break symmetries of Hamiltonian
- restore inversion, translational and rotational symmetry by projection on parity, linear and angular momentum

$$\underset{\sim}{P}^{\pi} = \frac{1}{2}(1 + \pi \underset{\sim}{\Pi})$$

$$\underset{\sim}{P}^{J}_{MK} = \frac{2J+1}{8\pi^2} \int d^3\Omega \, {D^{J}_{MK}}^{\star}(\Omega) \, \underset{\sim}{R}(\Omega)$$

$$\underset{\sim}{P}^{\mathbf{P}} = \frac{1}{(2\pi)^3} \int d^3X \; \exp\{-i(\underset{\sim}{\mathbf{P}} - \mathbf{P}) \cdot \mathbf{X}\}$$

PAV, VAP and Multiconfiguration

Projection After Variation (PAV)

- mean-field may break symmetries of Hamiltonian
- restore inversion, translational and rotational symmetry by projection on parity, linear and angular momentum

$$\underset{\sim}{P}^{\pi} = \frac{1}{2}(1 + \pi \underset{\sim}{\Pi})$$

$$\underset{\sim}{P}^{J}_{MK} = \frac{2J+1}{8\pi^2} \int d^3\Omega \, {D^{J}_{MK}}^{\star}(\Omega) \, \underset{\sim}{R}(\Omega)$$

$$\underset{\sim}{P}^{\mathbf{P}} = \frac{1}{(2\pi)^3} \int d^3X \; \exp\{-i(\underset{\sim}{\mathbf{P}} - \mathbf{P}) \cdot \mathbf{X}\}$$

Variation After Projection (VAP)

- effect of projection can be large
- **Variation after Angular Momentum and Parity Projection** (VAP) for light nuclei
- combine VAP with **constraints** on **radius**, **dipole** moment, **quadrupole** moment, . . . to generate additional configurations

PAV, VAP and Multiconfiguration

Projection After Variation (PAV)

- mean-field may break symmetries of Hamiltonian
- restore inversion, translational and rotational symmetry by projection on parity, linear and angular momentum

$$\underset{\sim}{P}^{\pi} = \frac{1}{2}(1 + \pi \underset{\sim}{\Pi})$$

$$\underset{\sim}{P}^{J}_{MK} = \frac{2J+1}{8\pi^2} \int d^3\Omega \, {D^{J}_{MK}}^{\star}(\Omega) \, \underset{\sim}{R}(\Omega)$$

Variation After Projection (VAP)

- effect of projection can be large
- **Variation after Angular Momentum and Parity Projection** (VAP) for light nuclei
- combine VAP with **constraints** on **radius**, **dipole** moment, **quadrupole** moment, . . . to generate additional configurations

$$\underset{\sim}{P}^{\mathbf{P}} = \frac{1}{(2\pi)^3} \int d^3X \; \exp\{-i(\underset{\sim}{\mathbf{P}} - \mathbf{P}) \cdot \mathbf{X}\}$$

Multiconfiguration Calculations

- **diagonalize** Hamiltonian in a set of projected intrinsic states

$$\left\{ \left| Q^{(a)} \right\rangle, \quad a = 1, \ldots, N \right\}$$

$$\sum_{K'b} \left\langle Q^{(a)} \middle| \underset{\sim}{H} \underset{\sim}{P}^{J^\pi}_{KK'} \underset{\sim}{P}^{\mathbf{P}=0} \middle| Q^{(b)} \right\rangle \cdot c^{\alpha}_{K'b} = E^{J^\pi \alpha} \sum_{K'b} \left\langle Q^{(a)} \middle| \underset{\sim}{P}^{J^\pi}_{KK'} \underset{\sim}{P}^{\mathbf{P}=0} \middle| Q^{(b)} \right\rangle \cdot c^{\alpha}_{K'b}$$

FMD vs NCSM model spaces

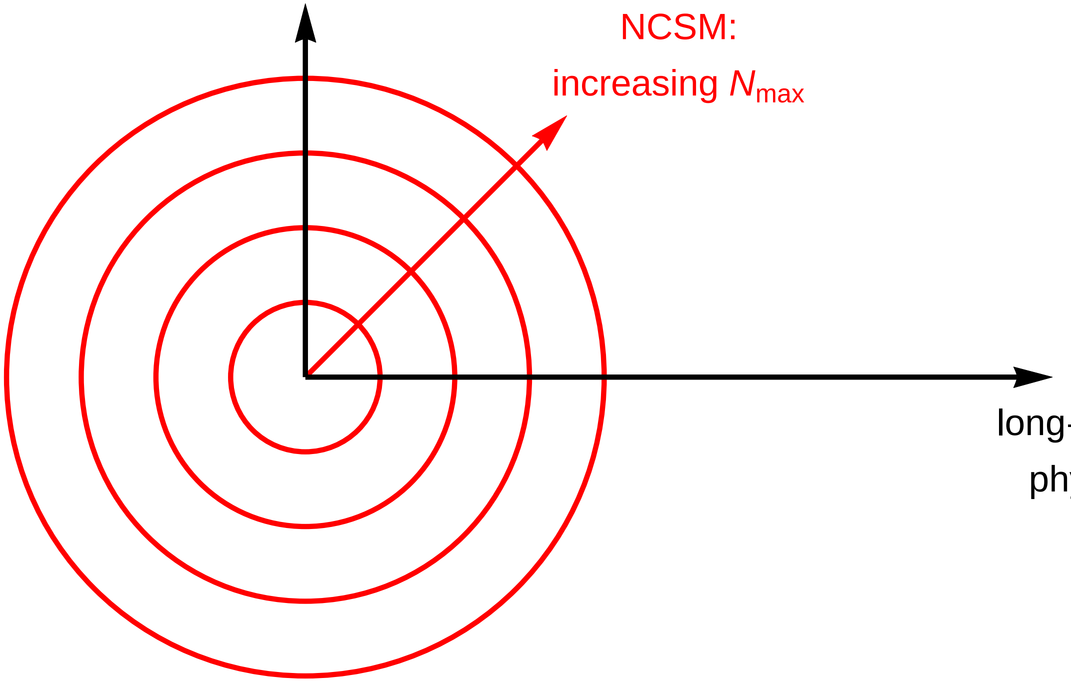

- NCSM allows good description of short-range physics, but long-range behavior suffers from harmonic oscillator asymptotics

FMD vs NCSM model spaces

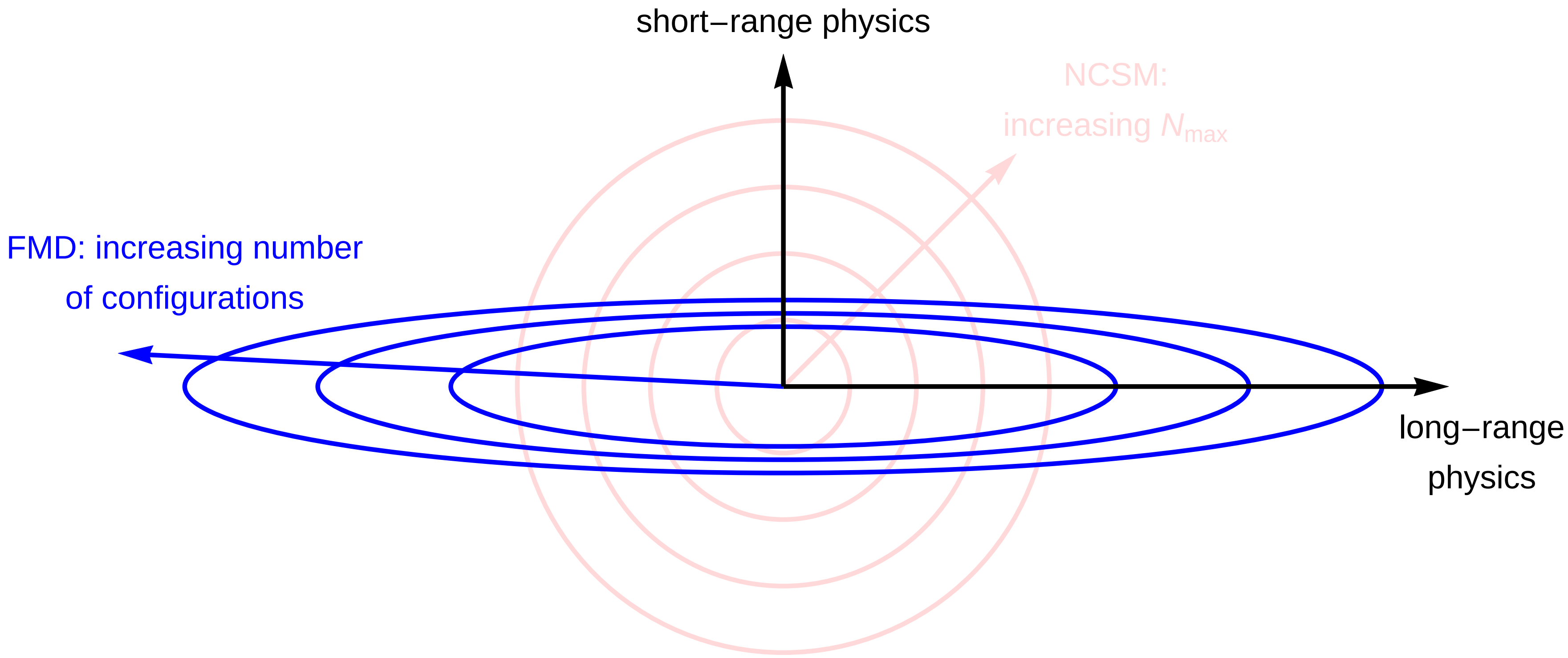

- NCSM allows good description of short-range physics, but long-range behavior suffers from harmonic oscillator asymptotics
- FMD allows to describe long-range physics by superposition of localized cluster configurations, but limited in description of short-range physics

Harmonic Oscillator $N\hbar\Omega$ Excitations

- FMD calulations predict an extended 3α-structure for the Hoyle state
- good agreement with elastic and inelastic electron scattering data

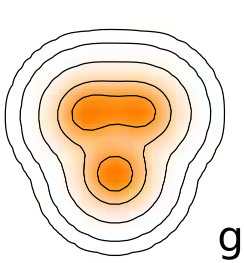

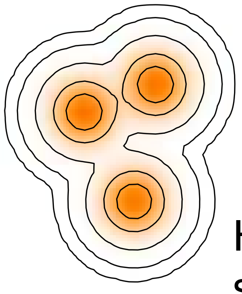

$$\mathrm{Occ}(N) = \langle\, \Psi \,|\, \delta\left(\textstyle\sum_i (\underset{\sim}{H}_i^{HO}/\hbar\Omega - 3/2) - N\right) |\, \Psi \,\rangle$$

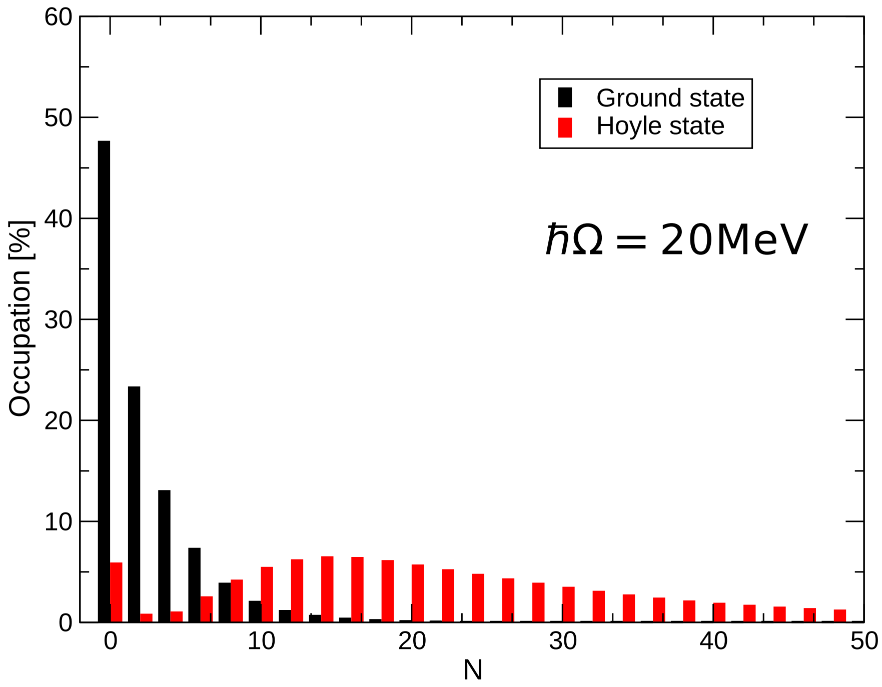

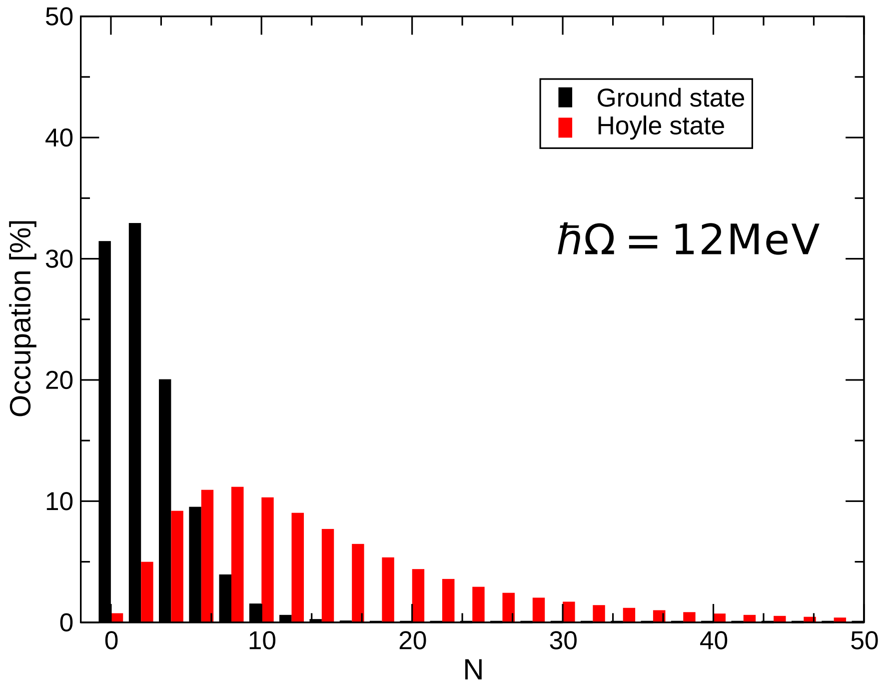

- Hoyle state very difficult to converge in no-core shell model

Chernykh, Feldmeier, Neff, von Neumann-Cosel, Richter, PRL **98**, 032501 (2007)

Neff, Feldmeier, Few-Body Syst. **45**, 145 (2009)

^{3}He(α,γ)^{7}Be radiative capture

one of the key reactions in the solar pp-chains

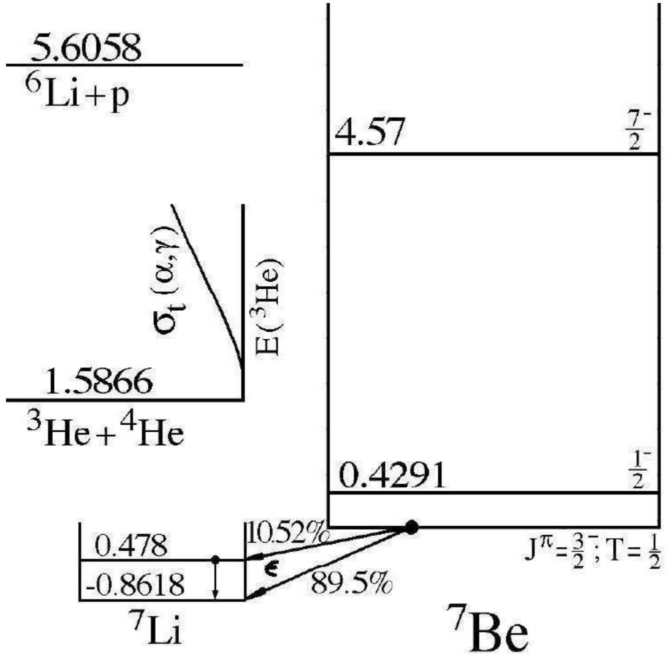

Effective Nucleon-Nucleon interaction:

UCOM(SRG) $\alpha = 0.20$ **fm**^{4} – $\lambda \approx 1.5$ **fm**$^{-1}$

Many-Body Approach:

Fermionic Molecular Dynamics

- **Internal region: VAP configurations with radius constraint**
- **External region: Brink-type cluster configurations**
- **Matching to Coulomb solutions: Microscopic *R*-matrix method**

Results:

- ^{7}Be **bound and scattering states**
- **Astrophysical *S*-factor**

T. Neff, Phys. Rev. Lett. **106**, 042502 (2011)

$^{3}He(\alpha,\gamma)^{7}Be$
FMD model space

Frozen configurations

- 15 antisymmetrized wave function built with ^{4}He and ^{3}He FMD clusters up to channel radius a=12 fm

Polarized configurations

- 30 FMD wave functions obtained by VAP on $1/2^-$, $3/2^-$, $5/2^-$, $7/2^-$ and $1/2^+$, $3/2^+$ and $5/2^+$ combined with radius constraint in the interaction region

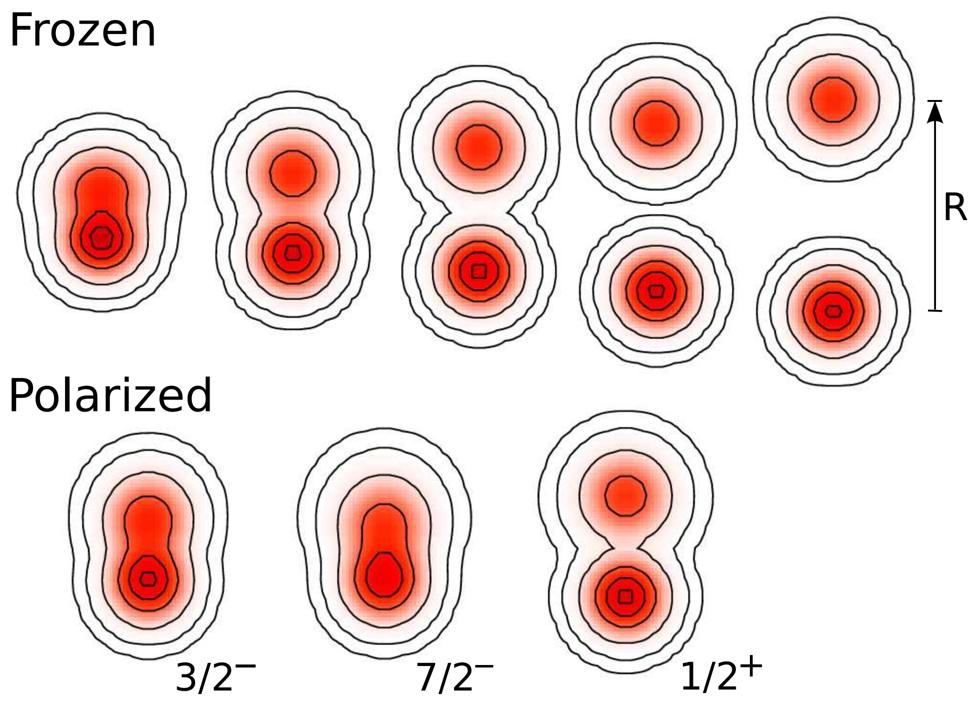

Boundary conditions

- Match relative motion of clusters at channel radius to Whittaker/Coulomb functions with the **microscopic *R*-matrix** method of the Brussels group

  D. Baye, P.-H. Heenen, P. Descouvemont

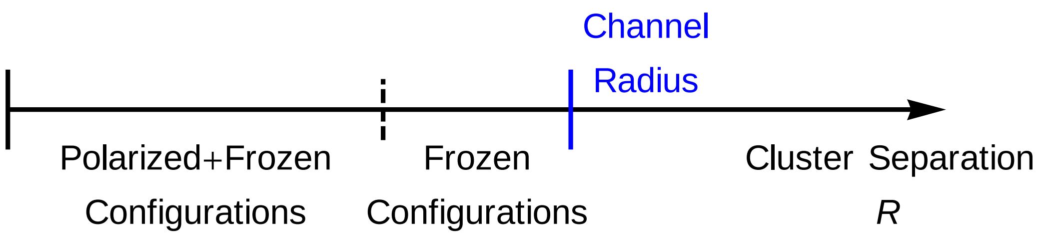

p-wave Bound and Scattering States

Bound states

		Experiment	FMD
^{7}Be	$E_{3/2-}$	-1.59 MeV	-1.49 MeV
	$E_{1/2-}$	-1.15 MeV	-1.31 MeV
	r_{ch}	2.647(17) fm	2.67 fm
	Q	–	-6.83 e fm^2
^{7}Li	$E_{3/2-}$	-2.467 MeV	-2.39 MeV
	$E_{1/2-}$	-1.989 MeV	-2.17 MeV
	r_{ch}	2.444(43) fm	2.46 fm
	Q	-4.00(3) e fm^2	-3.91 e fm^2

- centroid of bound state energies well described if polarized configurations included
- tail of wave functions tested by charge radii and quadrupole moments

Phase shift analysis:

Spiger and Tombrello, PR **163**, 964 (1967)

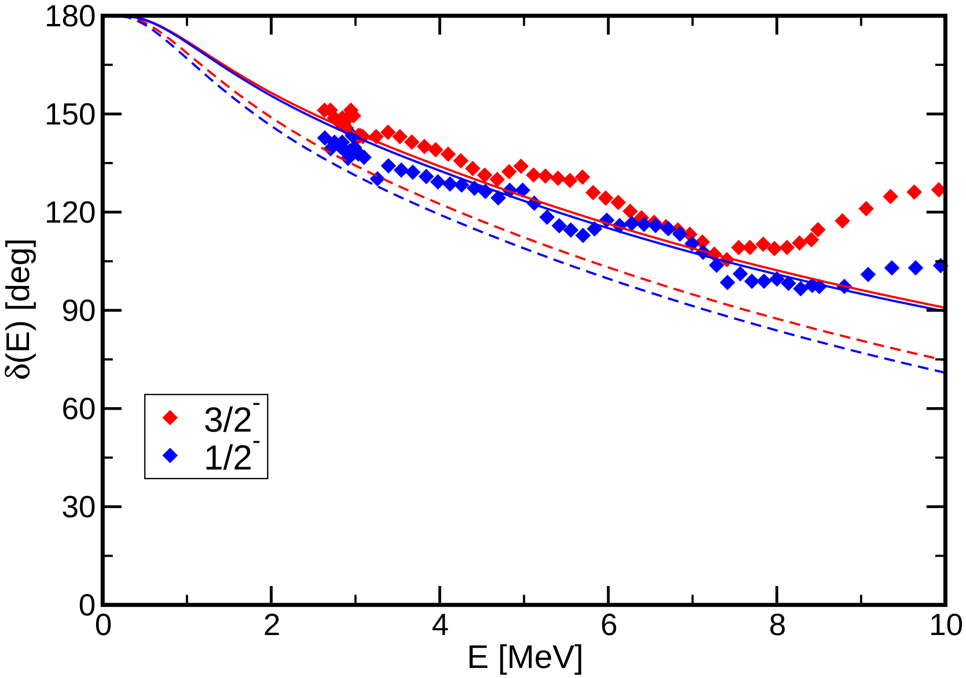

dashed lines – frozen configurations only

solid lines – polarized configurations in interaction region included

- Scattering phase shifts well described, polarization effects important

s-, *d*- and *f*-wave Scattering States

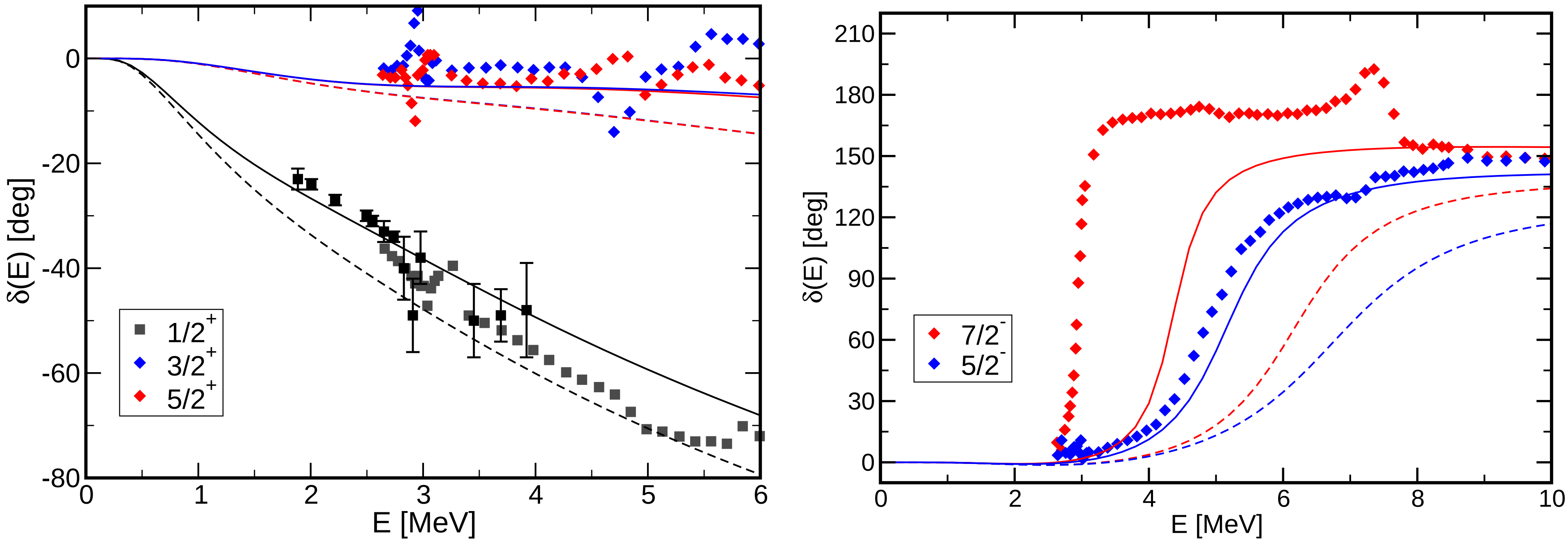

dashed lines – frozen configurations only – solid lines – FMD configurations in interaction region included

- polarization effects important
- *s*- and *d*-wave scattering phase shifts well described
- $7/2^-$ resonance too high, $5/2^-$ resonance roughly right, consistent with no-core shell model calculations

S-Factor

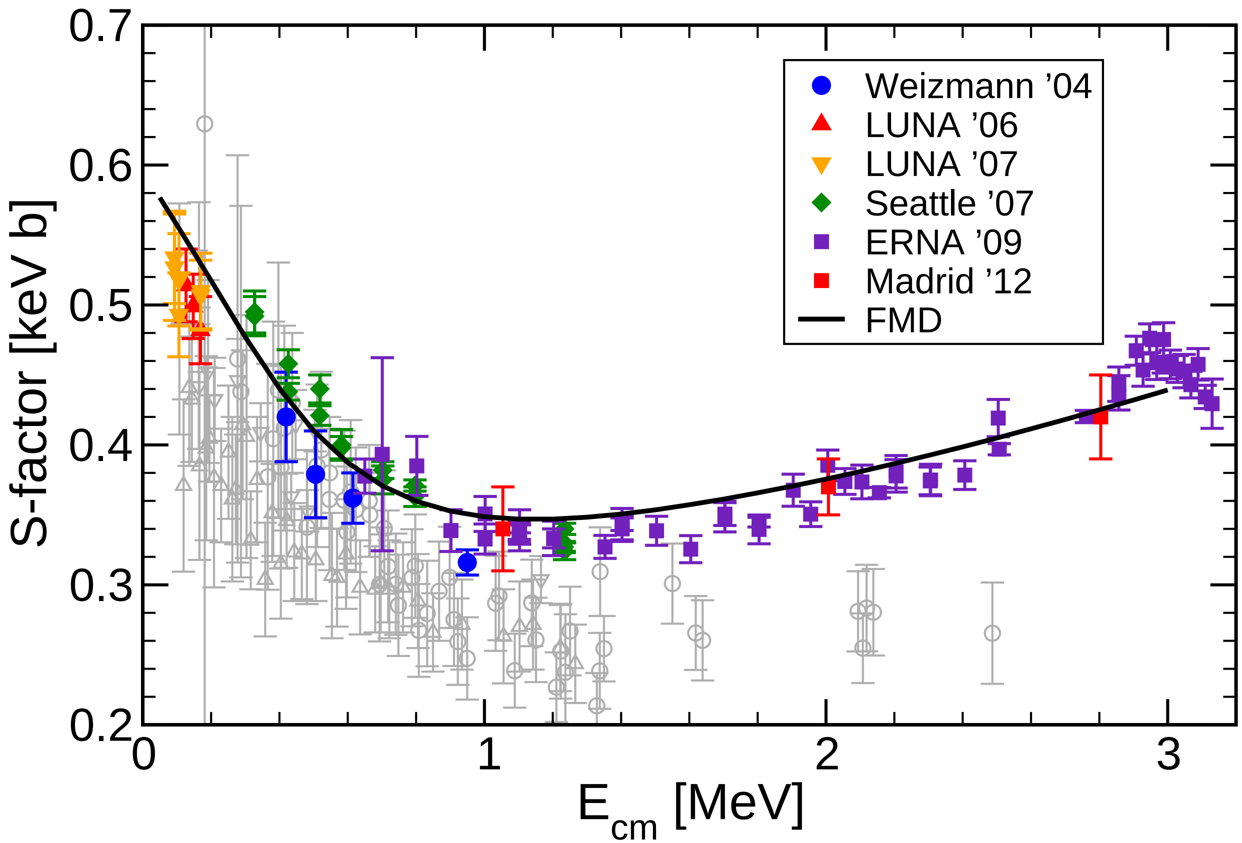

S-factor:

$$S(E) = \sigma(E) E \exp\{2\pi\eta\}$$

$$\eta = \frac{\mu Z_1 Z_2 e^2}{k}$$

Nara Singh *et al.*, PRL **93**, 262503 (2004)
Bemmerer *et al.*, PRL **97**, 122502 (2006)
Confortola *et al.*, PRC **75**, 065803 (2007)
Brown *et al.*, PRC **76**, 055801 (2007)
Di Leva *et al.*, PRL **102**, 232502 (2009)
Carmona-Gallardo *et al.*,
PRC **86**, 032801(R) (2012)

- dipole transitions from $1/2^+$, $3/2^+$, $5/2^+$ scattering states into $3/2^-$, $1/2^-$ bound states
- ➼ FMD is the only model that describes well the energy dependence and normalization of new high quality data
- ➼ fully microscopic calculation, bound and scattering states are described consistently

T. Neff, Phys. Rev. Lett. **106** (2011) 042502

Overlap Functions and Dipole Matrixelements

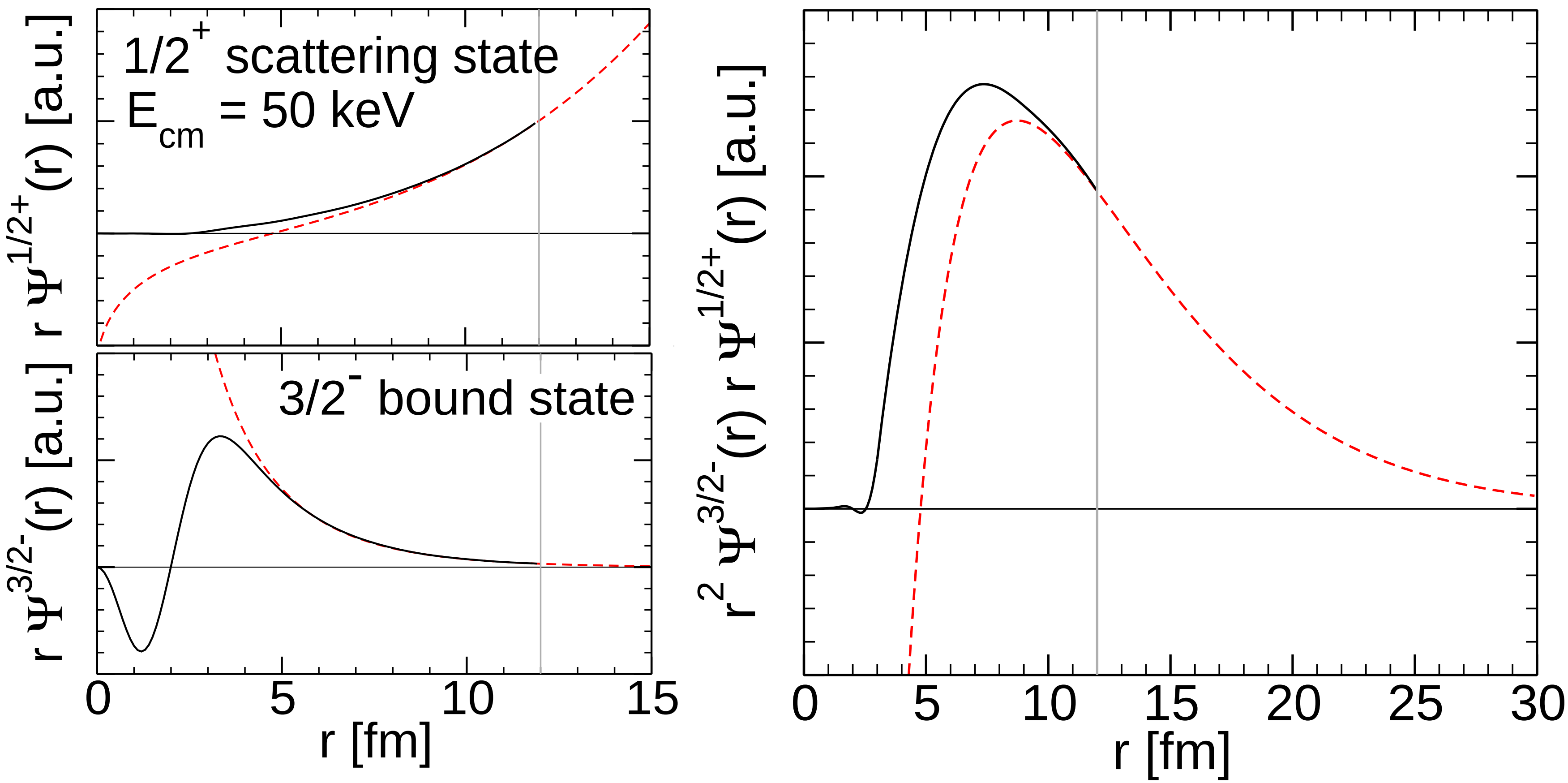

- Overlap functions from projection on RGM-cluster states
- Coulomb and Whittaker functions matched at channel radius a=12 fm
- Dipole matrix elements calculated from overlap functions reproduce full calculation within 2%
- cross section depends significantly on internal part of wave function, description as an "external" capture is too simplified

S-Factor

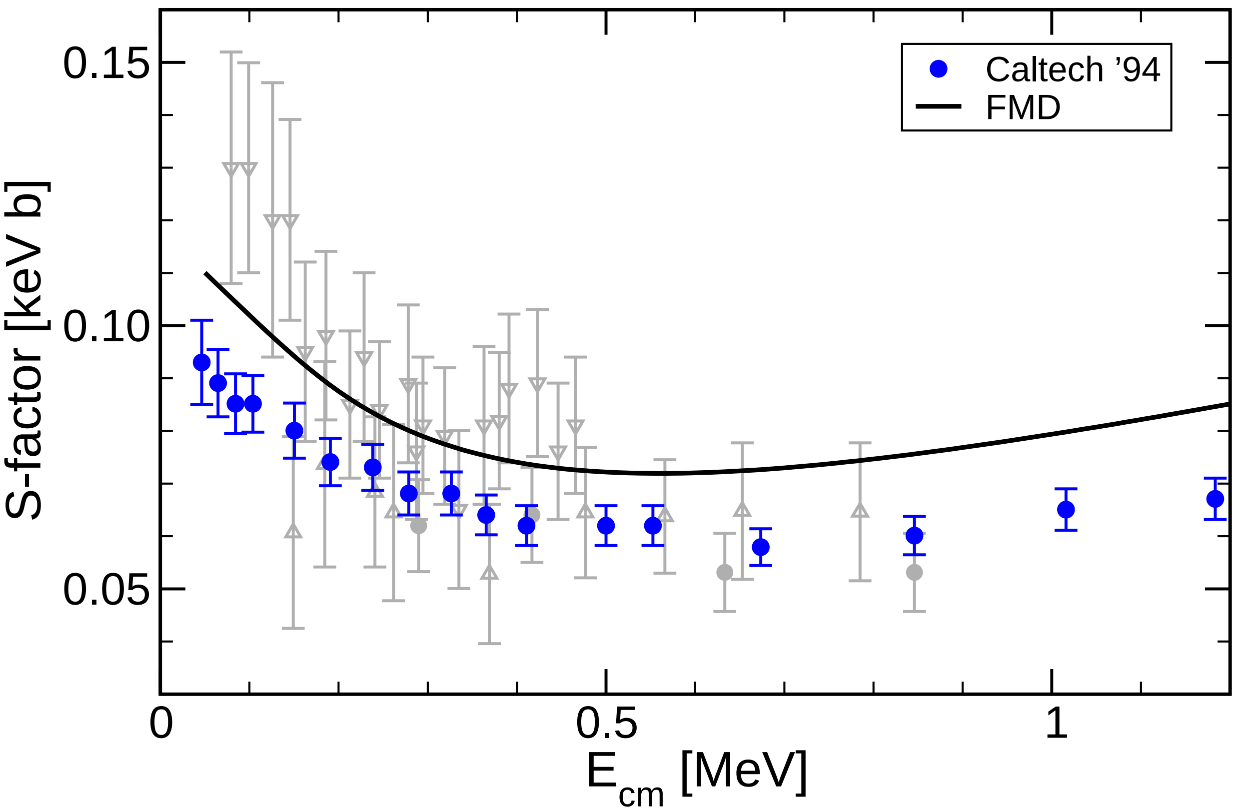

S-factor:

$$S(E) = \sigma(E)E\exp\{2\pi\eta\}$$

$$\eta = \frac{\mu Z_1 Z_2 e^2}{k}$$

Brune *et al.*, PRC **50**, 2205 (1994)

- isospin mirror reaction of $^3He(\alpha,\gamma)^7Be$
- ^7Li bound state properties and phase shifts well described

➸ FMD calculation describes energy dependence of Brune *et al.* data but cross section is larger by about 15%

S-Factor Contributions

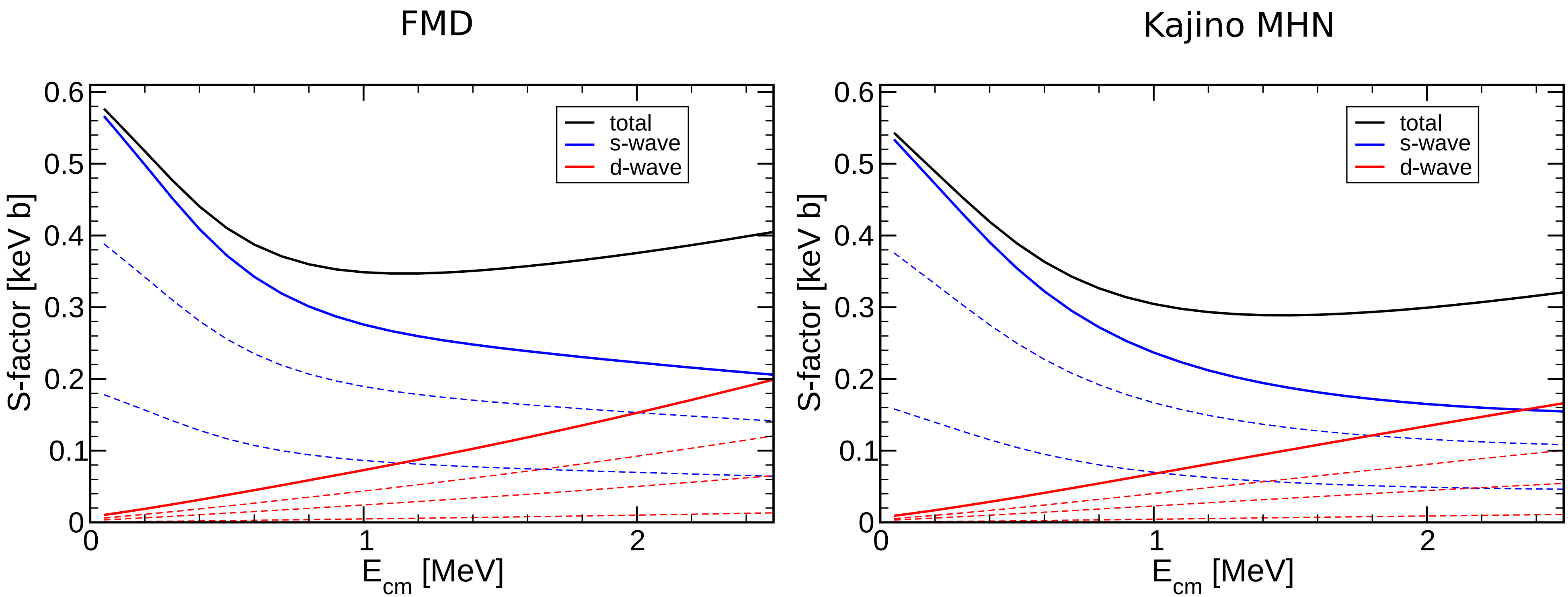

- main difference between FMD and Kajino results is originating in *s*-wave capture – both in normalization and energy dependence
- difference in normalization related to ground state properties – as seen in charge radius/quadrupole moment
- difference in energy dependence not understood yet
  – long-range of realistic interaction due to explicit description of pion-exchange ?
  – polarization of clusters in the interaction region ?

Beryllium Isotopes

Questions

- α**-clustering, halos in** ^{11}Be **and** ^{14}Be**,** $N = 8$ **shell closure ?**

Calculation

- **VAP and multiconfiguration-VAP calculations with mean proton distance as generator coordinate**
- **UCOM(SRG) effective spin-orbit strength is too small – modify interaction by multiplying spin-orbit interaction in** $S = 1$**,** $T = 1$ **channel with factor** $\eta \approx 2$

Observables

- **energies**
- **charge and matter radii, electromagnetic transitions**

Mean proton distance as generator coordinate

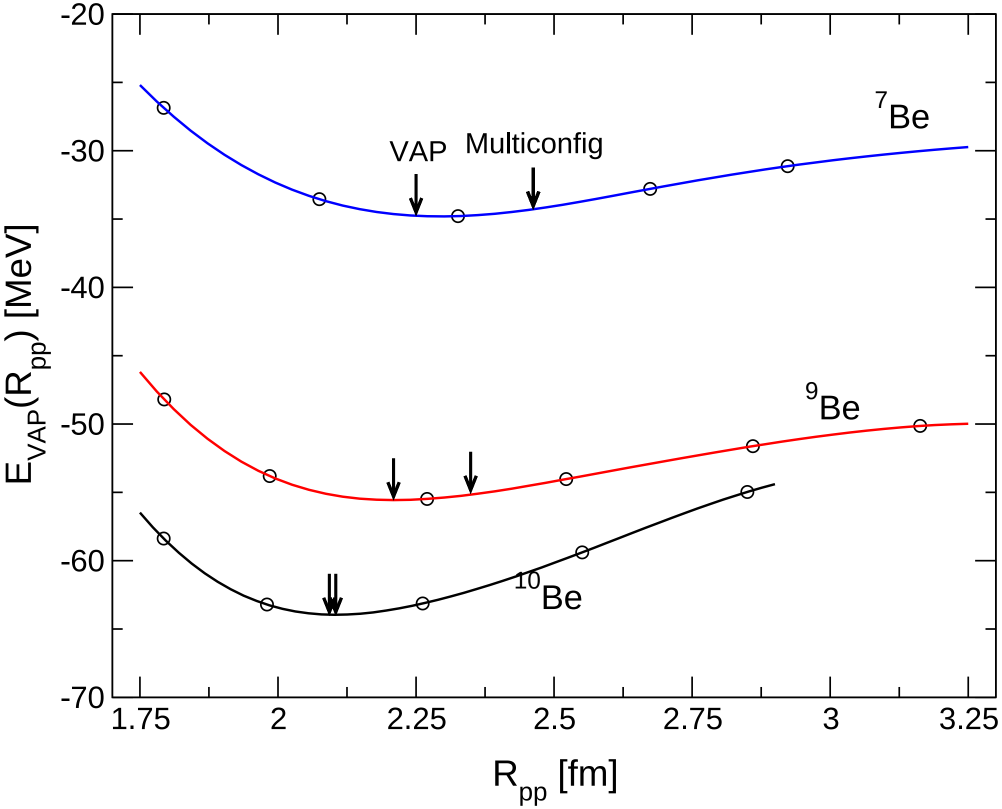

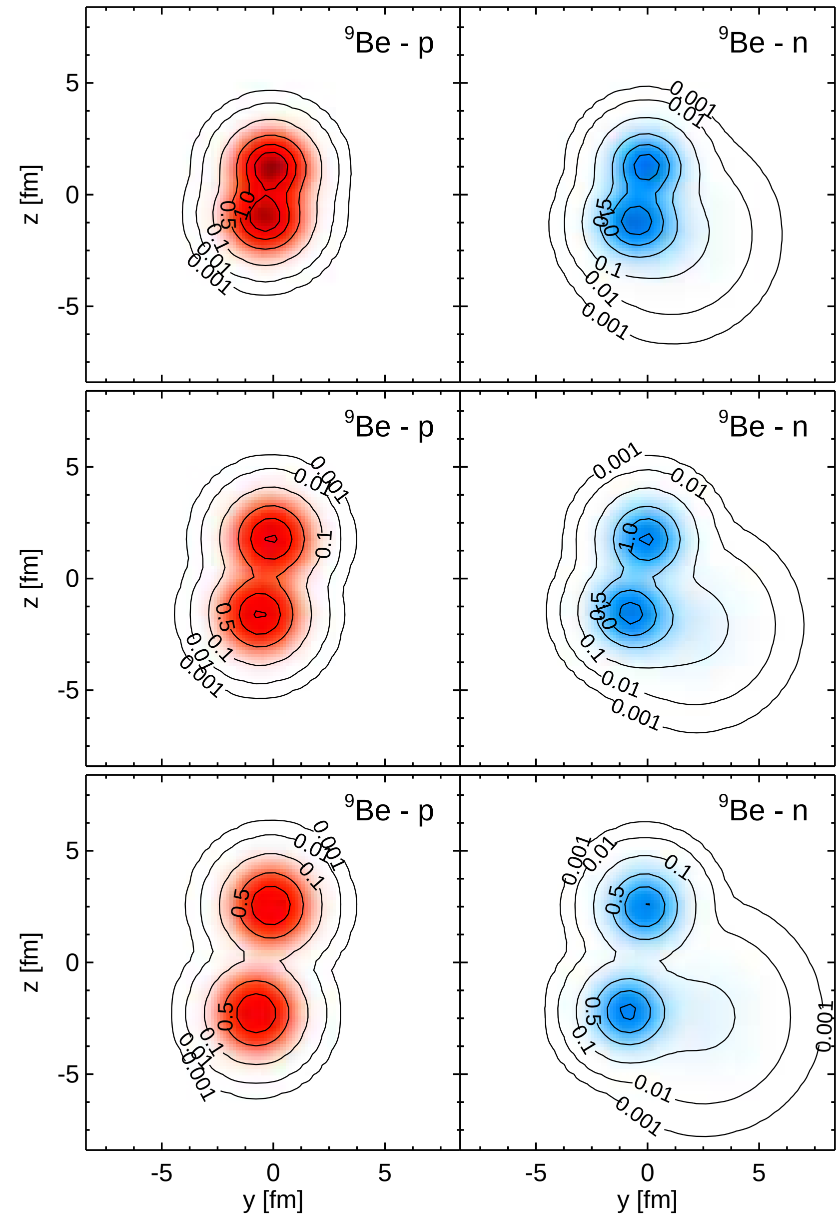

Mean proton distance

$$R_{pp}^2 = \frac{1}{Z^2} \langle \sum_{i<j}^{\text{protons}} (\mathbf{r}_i - \mathbf{r}_j)^2 \rangle$$

R_{pp} as a measure of
α-cluster distance

Mean proton distance as generator coordinate

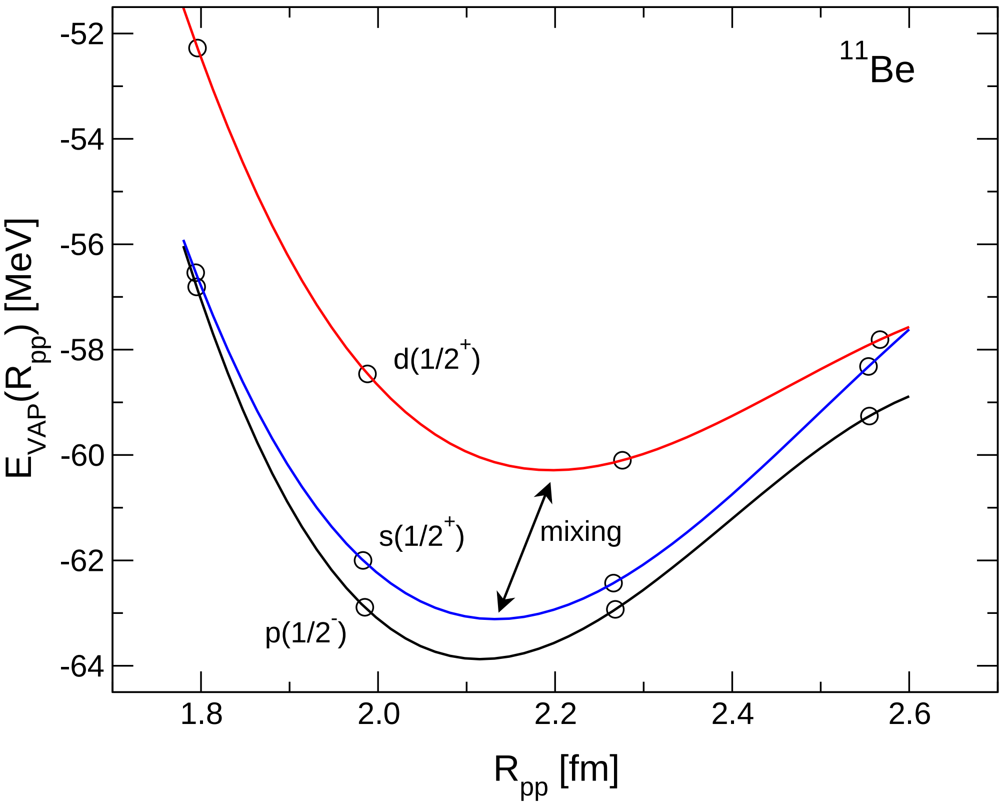

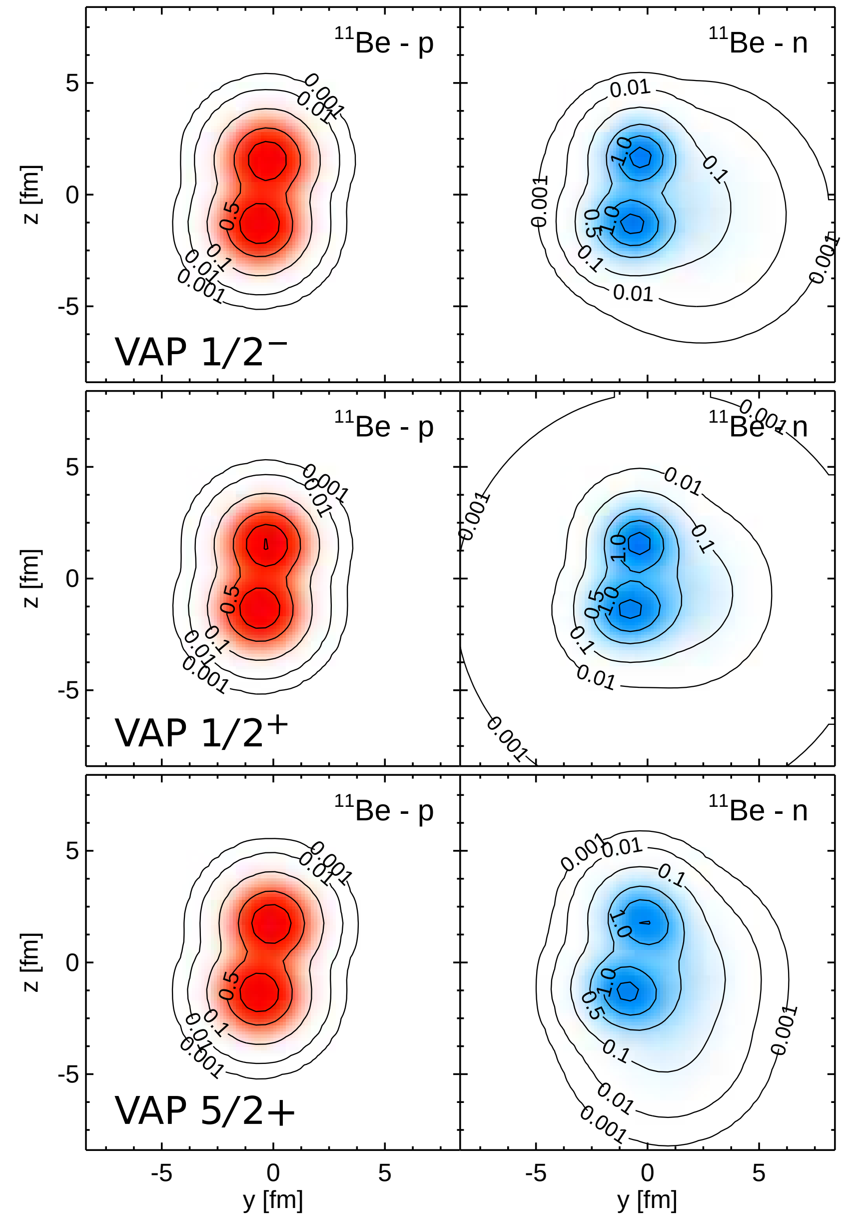

^{11}Be – "*p*", "*s*" and "*d*"-configurations

- "*s*"- and "*d*"-configurations will mix in $1/2^+$ state
- energy surfaces for "*p*" and "*s*" similar to those in ^{10}Be
- "*d*" surface has minimum at larger cluster distance → *d*-configuration has a polarized ^{10}Be core

$N = 8$ shell closure ?

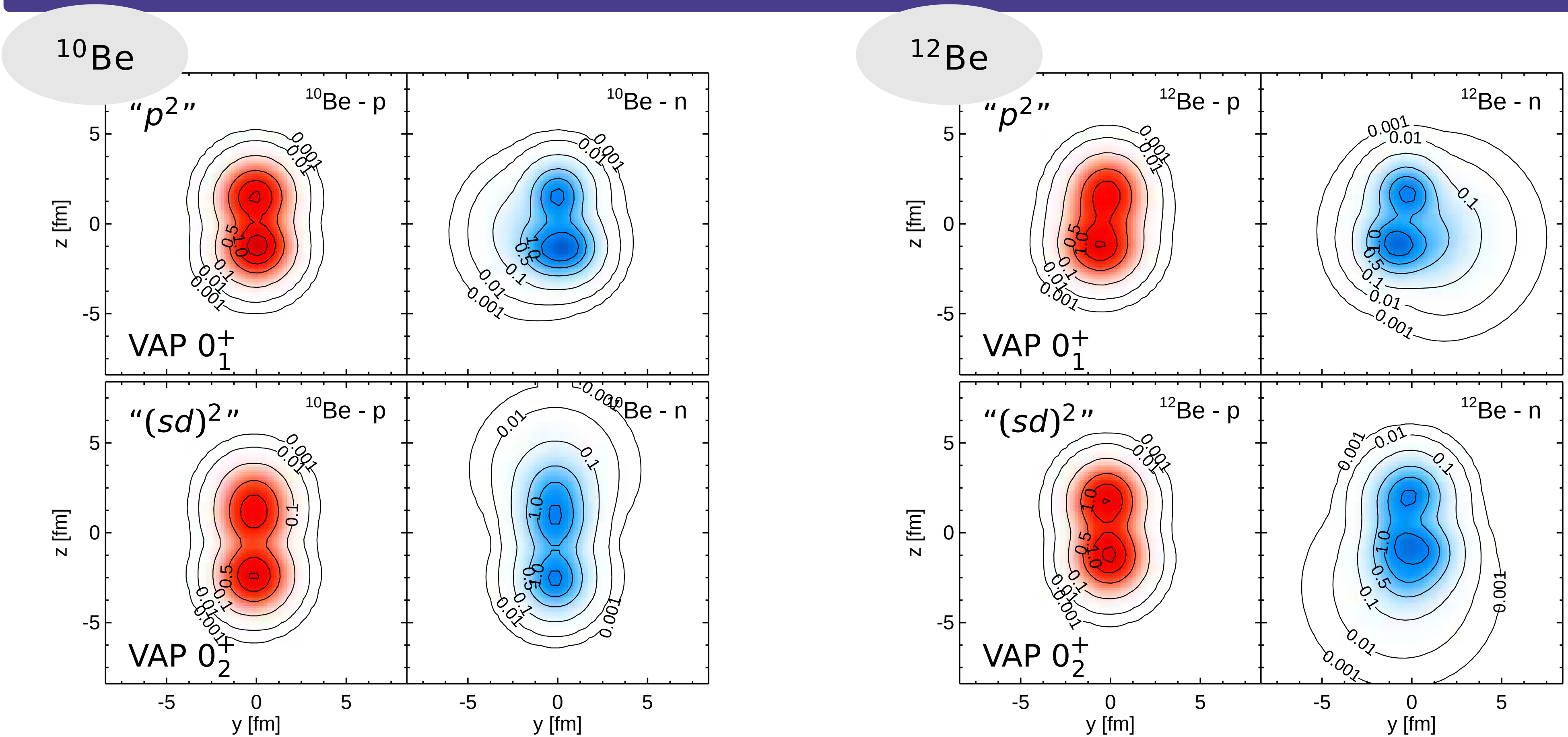

- in ^{12}Be normal and intruder configurations almost degenerate in energy
- contribution of spin-orbit force larger in intruder configuration
- eigenstate composition can be tuned from dominant p^2 to dominant $(sd)^2$ by changing spin-orbit factor from 2.0 to 2.2

Charge Radii

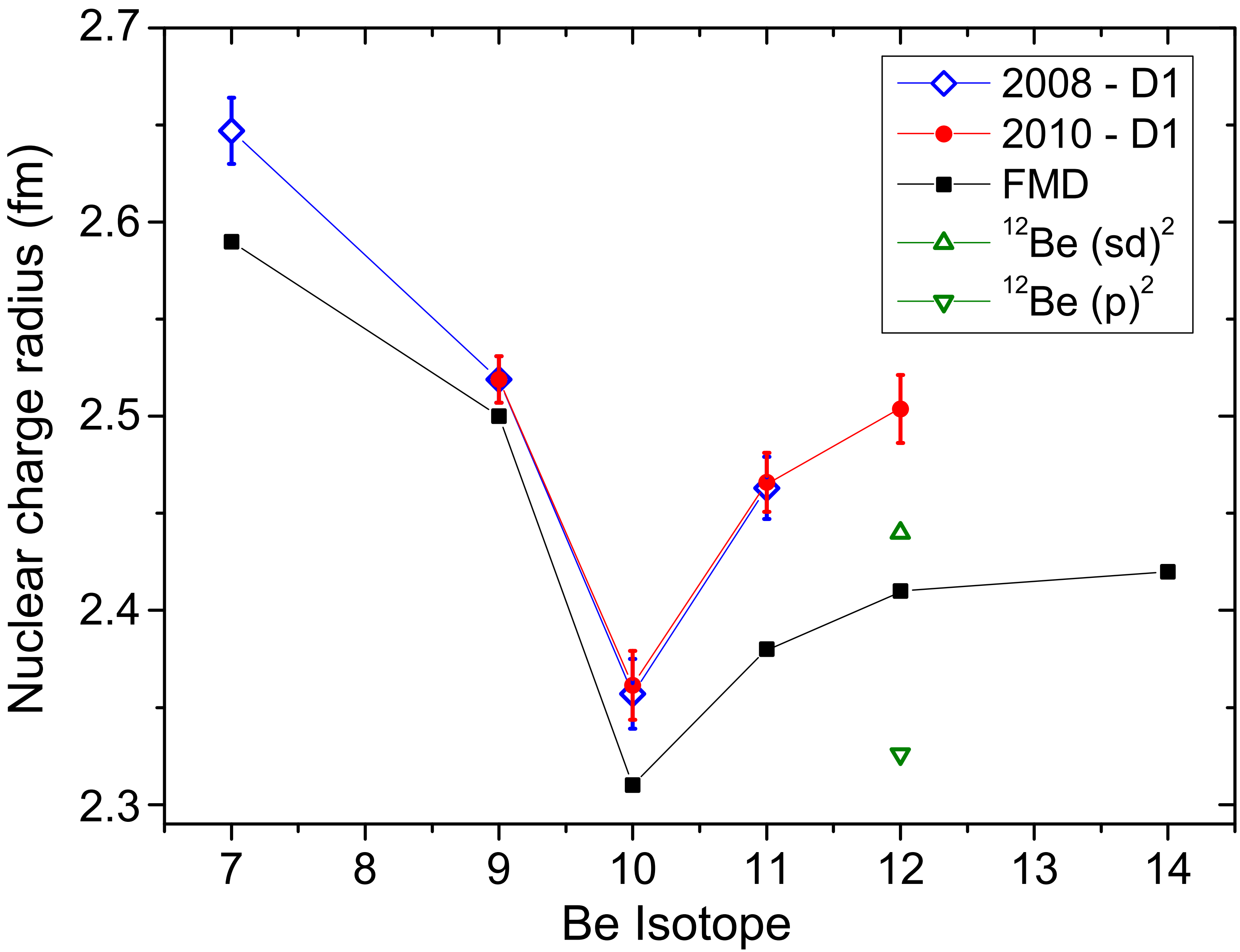

A. Krieger *et al.*, Phys. Rev. Lett. **108**, 142501 (2012)

Electromagnetic transitions

^{10}Be

	FMD(Multiconfig)	Experiment
$B(E2; 2_1^+ \to 0_1^+)$	$8.07\ e^2\text{fm}^4$	$9.2 \pm 0.3\ e^2\text{fm}^4$
$B(E2; 2_2^+ \to 0_1^+)$	$0.08\ e^2\text{fm}^4$	$0.11 \pm 0.02\ e^2\text{fm}^4$
$B(E2; 0_2^+ \to 2_1^+)$	$0.17\ e^2\text{fm}^4$	$3.2 \pm 1.9\ e^2\text{fm}^4$

^{12}Be

	FMD(Multiconfig)	Experiment
$B(E2; 2_1^+ \to 0_1^+)$	$8.75\ e^2\text{fm}^4$	$8.0 \pm 3.0\ e^2\text{fm}^4$
$B(E2; 0_2^+ \to 2_1^+)$	$7.45\ e^2\text{fm}^4$	$7.0 \pm 0.6\ e^2\text{fm}^4$
$M(E0; 0_1^+ \to 0_2^+)$	$0.90\ e\text{fm}^2$	$0.87 \pm 0.03\ e\text{fm}^2$

- Monopole and Quadrupole transitions directly connected to mixing between normal and intruder configurations
- 2_1^+ state has dominant intruder contribution

McCutchan *et al.*. Phys. Rev. Lett. **103**, 192501 (2009).
Nakamura *et al.*, Phys. Lett. **B394**, 11 (1997).
Shimoura *et al.*, Phys. Lett. **B654**, 87 (2007).
Iwasaki *et al.*, Phys. Lett. **B491**, 8 (2000).

Summary

Unitary Correlation Operator Method

- Realistic low-momentum interaction V_{UCOM}

Fermionic Molecular Dynamics

- Microscopic many-body approach using Gaussian wave-packets
- Projection and multiconfiguration mixing

^{3}He(α,γ)^{7}Be Radiative Capture

- Bound states, resonance and scattering wave functions
- S-Factor: energy dependence and normalization

Beryllium Isotopes

- Breakdown of $N = 8$ shell closure
- Charge radii

Thanks to my collaborators:
Hans Feldmeier (GSI), Wataru Horiuchi (Hokkaido), Karlheinz Langanke (GSI), Robert Roth (TUD), Yasuyuki Suzuki (Niigata), Dennis Weber (GSI)